Mercury isotopes as tracers of ecology and metabolism in two sympatric shark species

Gaël Le Croizier, Anne Lorrain, Jeroen E. Sonke, Sébastien Jaquemet, Gauthier Schaal, Marina Renedo, Lucien Besnard, Yves Cherel, David Point

HAL Id: hal-02871364
https://hal.science/hal-02871364

Submitted on 4 Jan 2021

Journal Pre-proof

Mercury isotopes as tracers of ecology and metabolism in two sympatric shark species

Gaël Le Croizier, Anne Lorrain, Jeroen E. Sonke, Sébastien Jaquemet, Gauthier Schaal, Marina Renedo, Lucien Besnard, Yves Cherel, David Point

Gaël Le Croizier: Conceptualization, Methodology, Formal analysis, Writing - Original Draft, Writing - Review & Editing. **Anne Lorrain**: Resources, Writing - Review & Editing, Supervision, Funding acquisition. **Jeroen Sonke**: Formal analysis, Resources, Writing - Review & Editing, Supervision, Funding acquisition. **Sébastien Jaquemet**: Investigation, Resources, Writing - Review & Editing, Funding acquisition. **Gauthier Schaal**: Conceptualization, Writing - Review & Editing. **Marina Renedo**: Writing - Review & Editing. **Lucien Besnard**: Writing - Review & Editing. **Yves Cherel**: Resources, Writing - Review & Editing. **David Point**: Resources, Writing - Review & Editing, Supervision, Funding acquisition.
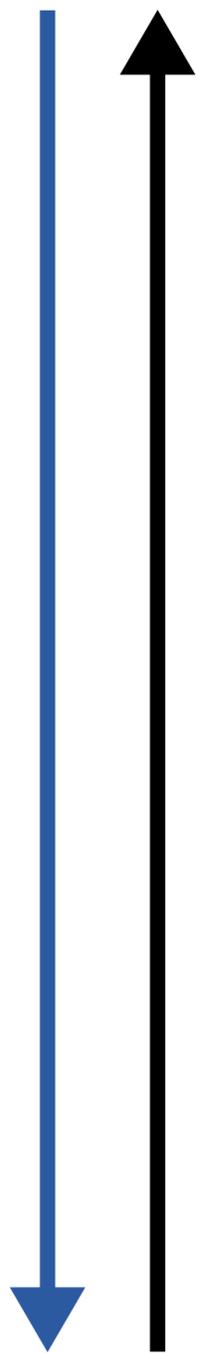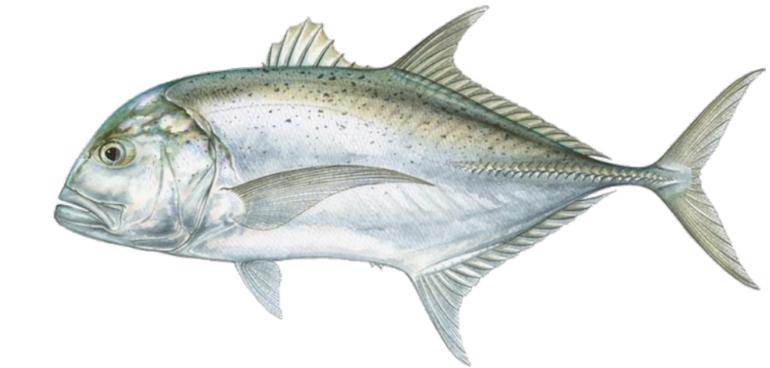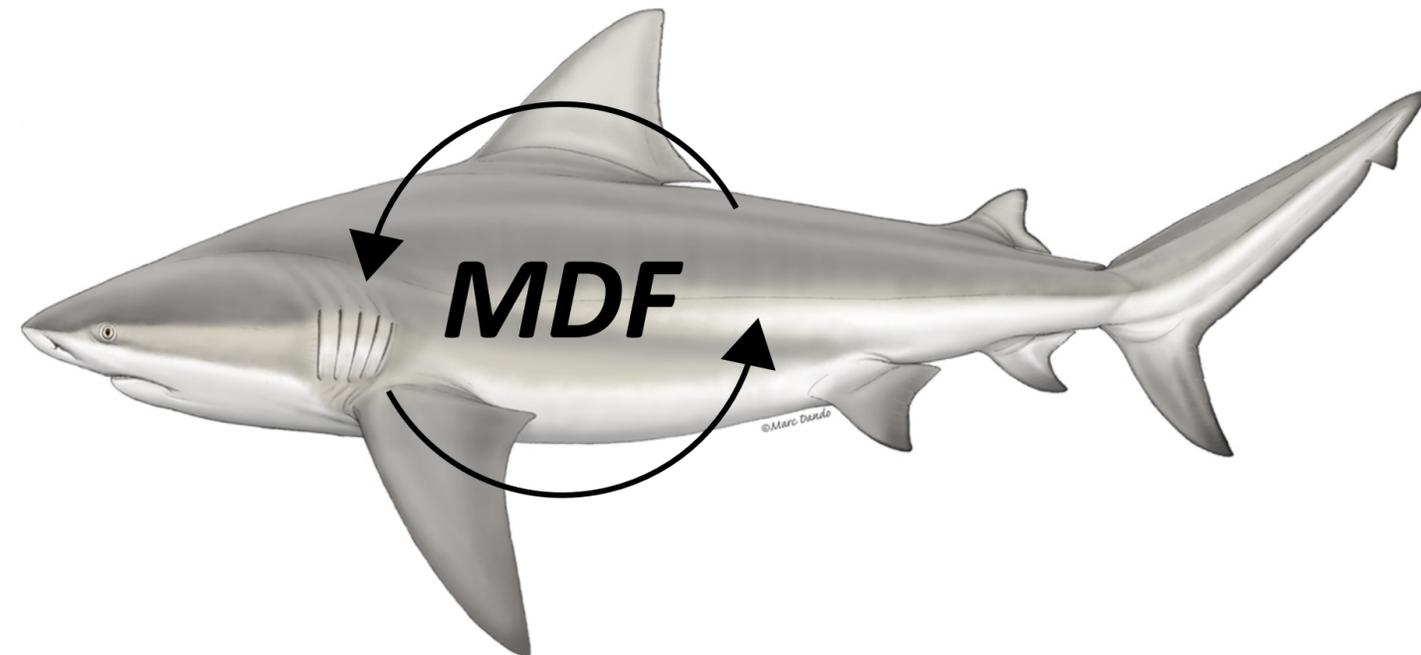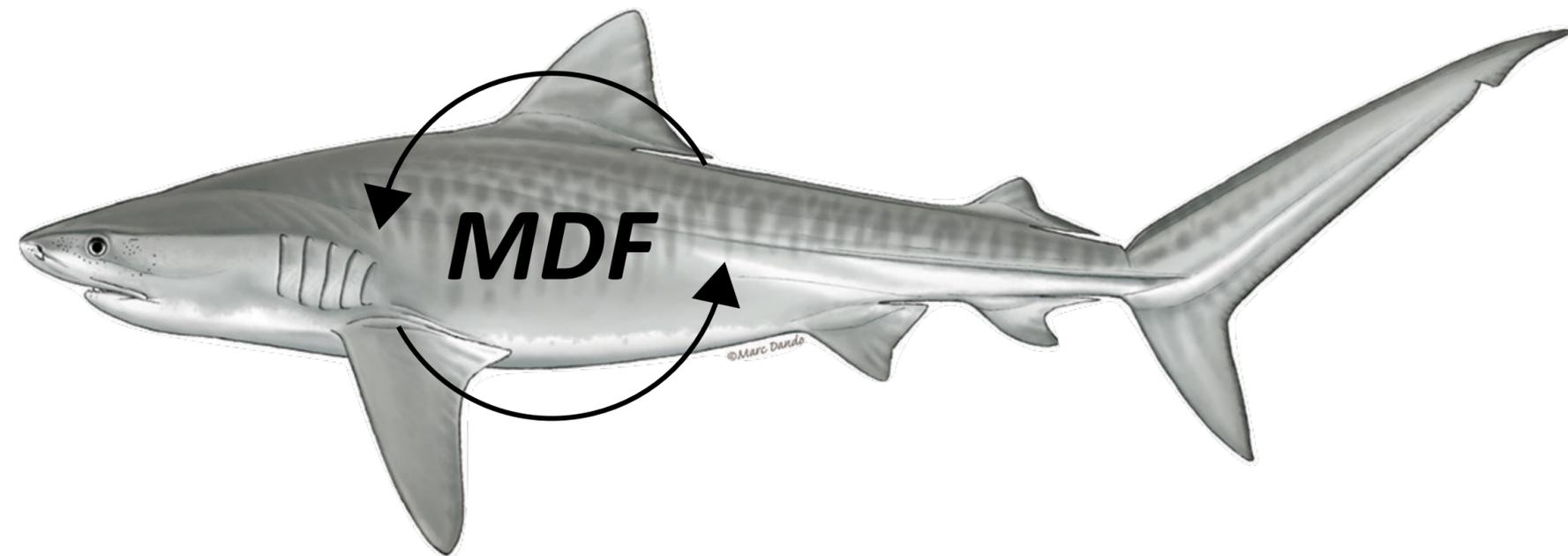
Mercury isotopes as tracers of ecology and metabolism in two sympatric shark species

Gaël Le Croizier[1][*], Anne Lorrain[2], Jeroen E. Sonke[1], Sébastien Jaquemet[3], Gauthier Schaal[2], Marina Renedo[1], Lucien Besnard[2], Yves Cherel[4], David Point[1].

[1]Géosciences Environnement Toulouse (GET), Observatoire Midi Pyrénées (OMP), UMR 5563 CNRS/IRD/Université Paul Sabatier, 14 avenue Edouard Belin, 31400 Toulouse, France

[2]Laboratoire des Sciences de l'Environnement Marin (LEMAR), UMR 6539 CNRS/UBO/IRD/IFREMER, BP 70, 29280 Plouzané, France

[3]Laboratoire ENTROPIE, UMR 9220 CNRS/IRD/Université de La Réunion, 15 Avenue René Cassin, BP 92003, 97744 Saint-Denis, La Réunion, France

[4]Centre d'Etudes Biologiques de Chizé (CEBC), UMR 7372 du CNRS-La Rochelle Université, 79360 Villiers-en-Bois, France

ORCID numbers: 0000-0002-5093-8406 (G. Le Croizier), 0000-0001-7146-3035 (J. Sonke), 0000-0003-4199-4657 (S. Jaquemet), 0000-0003-3860-1517 (G. Schaal), 0000-0002-9224-8745 (M. Renedo), 0000-0001-9469-9489 (Y. Cherel), 0000-0002-1289-2072 (A. Lorrain), 0000-0002-5218-7781 (D. Point)

*Corresponding author: gael.lecroizier@ird.fr

1 ABSTRACT

2 In coastal ecosystems, top predators are exposed to a wide variety of nutrient and

3 contaminant sources due to the diversity of trophic webs within coastal areas. Mercury

4 contamination could represent an additional threat to shark populations that are declining

5 worldwide. Here we measured total mercury, carbon and nitrogen isotopes as well as

6 mercury isotopes in two co-occurring shark species (the bull shark *Carcharhinus leucas* and

7 the tiger shark *Galeocerdo cuvier*) and their prey from a coastal ecosystem of the western

8 Indian Ocean (La Réunion Island), to (i) determine their main trophic Hg source and (ii)

9 better characterize their diet composition and foraging habitat. Hg isotope signatures

10 (Δ^{199}Hg and δ^{202}Hg) of shark prey suggested that bull sharks were exposed to methylmercury

11 (MeHg) produced in the water column while tiger sharks were exposed to mesopelagic

12 MeHg with additional microbial transformation in slope sediments. Δ^{199}Hg values efficiently

13 traced the ecology of the two predators, demonstrating that bull sharks targeted coastal

14 prey in shallow waters while tiger sharks were mainly foraging on mesopelagic species in the

15 slope deeper waters. Unexpectedly, we found a positive shift in δ^{202}Hg (> 1‰) between

16 sharks and their prey, leading to high δ^{202}Hg values in the two shark species (e.g. 1.91 ± 0.52

17 ‰ in the bull shark). This large shift in δ^{202}Hg indicates that sharks may display strong MeHg

18 demethylation abilities, possibly reflecting evolutionary pathways for mitigating their MeHg

19 contamination.

20

21

1. Introduction

22

23   Mercury (Hg) contamination constitutes a major global environmental concern,

24   resulting in deleterious effects on marine organisms due to exposure to the toxic

25   methylmercury (MeHg) form (Cáceres-Saez et al., 2018; Krey et al., 2015; Scheuhammer et

26   al., 2015). Located at the interface between the atmosphere, lands, rivers and oceans,

27   coastal areas are exposed to a wide variety of Hg sources and are at the same time used

28   extensively and increasingly for a large number of activities, including resources exploitation

29   or tourism. Within these complex ecosystems, long-lived organisms at the top of food webs

30   usually display the highest Hg levels, due to bioaccumulation and biomagnification

31   processes, which correspond to the increase of MeHg and other contaminant concentration

32   over time and with the trophic position, respectively. Populations of marine predators are

33   declining worldwide (Baum et al., 2003; Ferretti et al., 2008; Myers and Worm, 2003),

34   including coastal sharks (Hammerschlag et al., 2019; Roff et al., 2018). The harmful effects of

35   MeHg could thus represent an additional threat to the most depleted shark populations.

36   The bull shark *Carcharhinus leucas* and the tiger shark *Galeocerdo cuvier* are among

37   the largest marine top-predators, playing a key role in tropical marine ecosystems (Roff et

38   al., 2016). Due to their high trophic position and long life span, they are known to

39   accumulate high MeHg levels (McKinney et al., 2016). The two species can be temporarily

40   sympatric (i.e. co-occurring) in coastal ecosystems, but they also exhibit different habitat use

41   involving incursions in freshwater and strong affinity for coral reefs for the bull shark

42   (Espinoza et al., 2016; Matich and Heithaus, 2015; Werry et al., 2012) and large offshore

43   movements for tiger sharks (James S. E. Lea et al., 2015; Meyer et al., 2018), during which

44   they can dive in deep waters (Afonso and Hazin, 2015). Despite similar trophic positions, the

45   two species demonstrate segregation in their feeding habitats. While bull sharks can show

46   high individual specialization and a strong dependence on coastal resources, tiger sharks are

47   generalist predators able to rely on both coastal and oceanic prey (Dicken et al., 2017;

48   Trystram et al., 2016).

49   Top predators using coastal ecosystems are known to feed on different food webs

50   (Bird et al., 2018), inducing exposure to different sources and concentrations of

51   contaminants (Le Croizier et al., 2016, 2019b). To characterize dietary resources, nitrogen

52   and carbon stable isotopes ($\delta^{15}N$ and $\delta^{13}C$) are traditionally used in ecotoxicological studies

53   (Le Bourg et al., 2019; Le Croizier et al., 2020), reflecting respectively the trophic position

54   (Pethybridge et al., 2018) and foraging habitat (Bird et al., 2018) of consumers. However,

55   these tools show limitations, such as the variability of N and C isotopic fractionation during

56   trophic transfers (Kim et al., 2012; Malpica-Cruz et al., 2012). More recently, new techniques

57   such as Hg stable isotope analyses have been applied to characterize the sources and

58   transfer routes of this contaminant (Gehrke et al., 2011; Sackett et al., 2017; Senn et al.,

59   2010).

60   In seawater, MeHg is subject to mass-independent fractionation ("MIF", generally

61   represented by $\Delta^{199}Hg$) under the influence of solar radiation, which induces a preferential

62   photochemical demethylation of the light and odd-mass isotopes. In the photic zone (i.e. the

63   part of the water column exposed to light), the remaining MeHg pool available to marine

64   organisms is therefore enriched in the heavy and odd-mass Hg isotopes. This process induces

65   a $\Delta^{199}Hg$ gradient from the surface (photic or epipelagic zone, between 0 and 200 m deep) to

66   depth (twilight or mesopelagic zone, between 200 and 1000 m deep), with higher $\Delta^{199}Hg$

67   values near the surface. This isotopic gradient allows to trace the vertical foraging habitat of

4

68　marine consumers (Blum et al., 2013; Madigan et al., 2018; Sackett et al., 2017). Moreover,

69　Δ^{199}Hg constitutes a trophic tracer of major interest since Δ^{199}Hg values are conserved

70　between prey and predators due to the absence of MIF during trophic interactions or

71　metabolic processes (Kwon et al., 2016, 2012; Masbou et al., 2018).

72　　Hg isotopes are also subject to mass-dependent fractionation ("MDF", generally

73　represented by δ^{202}Hg) that takes place during physico-chemical processes such as

74　photoreduction (Bergquist and Blum, 2007) and volatilization (Zheng et al., 2007), but also

75　during biological processes such as methylation (Janssen et al., 2016) and demethylation

76　(Perrot et al., 2016). δ^{202}Hg can be used to assess the Hg metabolism, such as the

77　transformation of MeHg into less toxic inorganic Hg (iHg) by demethylation in the liver of

78　marine organisms (Bolea-Fernandez et al., 2019). Indeed, the preferential demethylation of

79　light Hg isotopes induces an increase in δ^{202}Hg in the remaining MeHg pool which is

80　ultimately accumulated in other tissues such as muscle (Perrot et al., 2016). Thereby,

81　significant enrichment of δ^{202}Hg is generally found in mammal muscle and human hair

82　relative to trophic Hg sources, reflecting in vivo demethylation of MeHg (Laffont et al., 2011;

83　Li et al., 2014; Perrot et al., 2012).

84　　In the western Indian Ocean, only a few studies have documented Hg concentrations

85　in coastal species (Le Bourg et al., 2019; Sardenne et al., 2017), with most studies focusing

86　on offshore organisms (Bodin et al., 2017; Kiszka et al., 2015). In addition to trophic position

87　and body length, foraging habitat was found to influence Hg levels in various shark species

88　sampled across different locations in the southwestern Indian Ocean, including La Réunion

89　Island (Le Bourg et al., 2019). Indeed, higher Hg concentrations were observed in offshore

90　and deep-sea species compared to coastal species, suggesting different sources of MeHg

91   exposure between sharks feeding in nearshore shallow waters and those feeding in offshore

92   deep waters (Kiszka et al., 2015; Le Bourg et al., 2019). On the other hand, high Hg

93   concentrations were found in large coastal shark species from the east coast of South-Africa

94   without apparent influence of foraging depth (McKinney et al., 2016). The role of feeding

95   depth in MeHg exposure therefore remains to be clarified for predators using nearshore

96   ecosystems in the western Indian Ocean. Moreover, while hepatic demethylation of MeHg is

97   well known in marine mammals (Bolea-Fernandez et al., 2019; Perrot et al., 2016), bony fish

98   do not appear to have such metabolic capacities. Although it has recently been suggested

99   that sharks may have protective mechanisms that mitigate Hg toxicity (Merly et al., 2019), to

100   date there is no evidence of MeHg demethylation in sharks.

101   In this context, the present study focused on two sympatric predator species, the bull

102   and the tiger shark, sampled in a coastal ecosystem of the Indian Ocean (La Réunion Island).

103   The two major objectives were to:

104   1) Use Hg MIF signatures (Δ^{199}Hg values) as diet and foraging depth tracers to

105   determine whether different MeHg sources contribute to MeHg burdens in the two

106   shark species.

107   2) Use Hg MDF signatures (δ^{202}Hg values) as tracers of Hg metabolism to evaluate the

108   MeHg demethylation abilities in sharks.

109

2. Material and methods

111   **2.1 Sampling**

6

112   The study was carried out in the coastal ecosystem of La Réunion Island, an oceanic

113   island located in the southwestern Indian Ocean. The island is of volcanic origin and its

114   topography is characterized by abrupt slopes inducing close proximity between coastal and

115   offshore ecosystems. This remote island is far from continental masses and therefore far

116   from the main sources of industrial pollution.

117   Muscle samples from 20 bull sharks *Carcharhinus leucas* (10 males, 10 females) and 20 tiger

118   sharks *Galeocerdo cuvier* (8 males, 12 females) were collected from individuals caught by

119   local fishermen along the island slope on the west coast of La Réunion Island in 2015 (Figure

120   1). To minimize the impact of ontogenetic changes in diet and habitat on Hg isotope values,

121   most of the sharks were sub-adults and adults (i.e. > 259 cm for tiger sharks (Werry et al.,

122   2014) and > 160 cm for bull sharks (Werry et al., 2011) (SI Global dataset), and were thus

123   larger than the size at which dietary shifts occur (i.e. 200-230 cm for tiger sharks and 140 cm

124   for bull sharks) (Habegger et al., 2012; Lowe et al., 1996).

125   At La Réunion island, teleost fish species dominate the preys consumed by both bull

126   and tiger sharks, based on stomach contents (i.e. respectively 93% and 78% in terms of mass

127   percentage) (Trystram et al., 2016). However, the large diversity of prey (i.e. 56 and 148

128   species for bull and tiger sharks, respectively) (Trystram et al., 2016) makes it very difficult to

129   cover the full prey spectrum of sharks. In this context, we collected muscle samples from fish

130   with known ecology and representative of the different habitats that sharks could use for

131   foraging and by which Hg exposure could occur (SI Table S3). In a similar coastal ecosystem

132   (Hawaii, USA), terrestrial freshwater inputs to coastal sediments were previously identified

133   as the primary source of tissue Hg in the giant trevally *Caranx ignobilis* (Sackett et al., 2017).

134   In the present study, this fish species was then used as a proxy of Hg sources from the

7

135 demersal nearshore habitat. The yellow-edged lyretail *Variola louti*, a reef-associated

136 grouper was sampled here to represent the shallow coral ecosystem (Emslie et al., 2017)

137 while the great barracuda *Sphyraena barracuda* and the wahoo *Acanthocybium solandri*

138 were collected to represent the epipelagic nearshore habitat (Trystram, 2016). The

139 deepwater longtail red snapper *Etelis coruscans* was identified as primarily exposed to MeHg

140 through deepwater sediments (Sackett et al., 2017) and was thus used as a proxy of MeHg

141 sources from slope waters. Regarding pelagic offshore Hg sources, tuna species (i.e. the

142 yellowfin tuna *Thunnus albacares* and the skipjack tuna *Katsuwonus pelamis*) and the lantern

143 fish *Ceratoscopelus warmingii* were used as proxies of respectively epipelagic and

144 mesopelagic Hg sources, according to their known ecology and previously published Hg

145 isotope values (Blum et al., 2013; Madigan et al., 2018). *Ceratoscopelus warmingii* was

146 collected during the "La Pérouse" and "MAD-RIDGE-1" scientific cruises in 2016 aboard the

147 RV Antea off La Réunion Island and off southern Madagascar, respectively. All the other fish

148 species were sampled between January 2012 and December 2014 off the west coast of La

149 Réunion Island by local fishermen (Figure 1).

150 All samples were kept in a cool box following collection and thereafter frozen at −20 °C in

151 the laboratory until further analysis. Muscle samples were freeze-dried and ground into a

152 fine and homogeneous powder using an automated grinder.

153 **2.2 Muscle δ^{13}C and δ^{15}N values**

154   Urea and lipid extraction were not applied on shark samples. Although shark muscle

155 generally contains low lipid content (<1%) (Meyer et al., 2017), lipids are depleted in ^{13}C and

156 shark osmoregulatory strategy induce a significant urea retention which is depleted in ^{15}N.

157 This may cause bias in the interpretation of the δ^{13}C and δ^{15}N, and therefore requires a

158 mathematical normalization for the δ^{13}C and δ^{15}N values following urea and lipid extraction

159 in several species of sharks (Y. Li et al., 2016). Here, we applied the normalization equations

160 established for the bull and the tiger shark from La Réunion Island, for each species and each

161 sex (Martin and Jaquemet, 2019).

162 Approximately 0.5 mg of muscle were weighed and packed into tin capsules. Isotopic

163 composition (with a precision of 0.1‰ for both δ^{13}C and δ^{15}N) and carbon percentage and

164 nitrogen percentage content were measured at the Stable Isotope Laboratory, GNS Science,

165 Lower Hutt, New Zealand, using an Isoprime isotope ratio mass spectrometer interfaced to

166 an EuroEA elemental analyzer in continuous-flow mode (EA-IRMS). Results are expressed in

167 standard δ notation based on international standards (Vienna Pee Dee Belemnite for δ^{13}C

168 and atmospheric nitrogen for δ^{15}N) following the equation δ^{13}C or

169 δ^{15}N = [(Rsample / Rstandard) − 1] × 10^3 (in ‰), where R is ^{13}C/^{12}C or ^{15}N/^{14}N.

170 **2.3 Hg concentration and speciation**

171 Total Hg (THg) determination was carried out on an aliquot (around 20 mg) of dried

172 fish or shark muscle by combustion, gold trapping and atomic absorption spectrophotometry

173 detection using a DMA80 analyzer (Milestone, USA). Mercury concentrations in muscle

174 samples are expressed on a dry weight basis (µg·g^{-1} dw). Only one analysis was performed

175 per sample, but the accuracy and reproducibility of the method were established using two

176 freeze-dried certified biological materials: a tuna fish flesh homogenate reference material

177 (IAEA 436, IRMM) and a lobster hepatopancreas reference material (TORT 3, NRCC). The

178 certified values for IAEA 436 (4.19 ± 0.36 µg·g^{-1} dw) were reproduced (measured value:

179 4.20 ± 0.09 µg·g^{-1} dw, n=10) within the confidence limits. The certified values for TORT 3

9

180 (0.292 ± 0.022 µg·g^{-1} dw) were also reproduced (measured value: 0.286 ± 0.024 µg·g^{-1} dw,

181 n=10) within the confidence limits. The detection limit was 0.005 µg·g^{-1} dw.

182 THg is known to be almost exclusively in the MeHg form in shark and fish muscle

183 (Bosch et al., 2016; de Carvalho et al., 2014; Pethybridge et al., 2010; Ruiz-de-Cenzano et al.,

184 2014), including species sampled in this study (e.g. giant trevally and deepwater snapper

185 (Sackett et al., 2015), bull shark (Matulik et al., 2017)). However, a subset of muscle samples

186 from 10 bull sharks were analyzed for MeHg, specifically to verify that MeHg accounted for

187 the majority of THg in our shark muscle samples and to evaluate the link between δ^{202}Hg

188 values and Hg speciation. We focused on the bull shark, which showed the highest δ^{202}Hg

189 variability, and selected 5 individuals with the lowest δ^{202}Hg values and 5 sharks with the

190 highest δ^{202}Hg values (SI Figure S3). MeHg concentrations in shark samples were obtained by

191 the selective and quantitative extraction of MeHg followed by cold-vapor atomic

192 fluorescence spectroscopy (CV-AFS) determinations according to the procedure described by

193 (Masbou et al., 2013). MeHg fraction was expressed as the percentage of MeHg to THg ratio.

194 A tuna fish flesh homogenate reference material (BCR 464, IRMM) was tested to ensure

195 measurement accuracy and reproducibility, and a MeHg recovery of 95 ± 1% (n=2) was

196 obtained relative to certified concentration.

197 **2.4 Hg isotopes**

198 Aliquots of approximately 20 mg of dry muscle were left over night at room

199 temperature in 3 mL of concentrated bi-distilled nitric acid (HNO$_3$). Samples were then

200 digested on a hotplate for 6h at 85°C in pyrolyzed glass vessels closed by Teflon caps. One

201 mL of hydrogen peroxide (H$_2$O$_2$) was added and digestion was continued for another 6h at

202 85°C. One hundred µL of BrCl was then added to ensure a full oxidation of MeHg to inorganic

10

203   Hg. The digest mixtures were finally diluted in an inverse aqua regia (3 HNO3: 1 HCl, 20 vol.%

204   MilliQ water) to reach a nominal Hg concentration of 1 $ng \cdot g^{-1}$. Three types of certified

205   reference materials (TORT 3, BCR 464, IAEA 436) and blanks were prepared in the same way

206   as tissue samples (SI Table S1).

207   Mercury isotope compositions were measured at the Observatoire Midi-Pyrenées

208   using multicollector inductively coupled plasma mass spectrometry (MC–ICP–MS, Thermo

209   Finnigan Neptune Plus) with continuous-flow cold vapor (CV) generation using Sn(II)

210   reduction (CETAC HGX-200), according to a previously published method (Enrico et al., 2016;

211   Goix et al., 2019; Masbou et al., 2015). Hg isotope composition is expressed in δ notation

212   and reported in parts per thousand (‰) deviation from the NIST SRM 3133 standard, which

213   was determined by sample-standard bracketing according to the following equation: $\delta^{XXX}Hg$

214   (‰) = [($(^{XXX}Hg/^{198}Hg)_{sample}$ / $(^{XXX}Hg/^{198}Hg)_{NIST\ 3133}$) -1] X 1000

215   where xxx represents the mass of each mercury isotope. ^{204}Hg was not measured due to

216   limitations in MC-ICP-MS cup configuration. $\delta^{202}Hg$ is used as a measure of MDF. Measures

217   of MIF are calculated as the difference between a measured δ-value, and the predicted δ-

218   value that is calculated by multiplying the measured $\delta^{202}Hg$ value by the kinetic MDF

219   fractionation factor for each isotope (Bergquist and Blum, 2007). MIF is expressed by the Δ

220   notation:

221     $\Delta^{199}Hg$ (‰) = $\delta^{199}Hg$ – ($\delta^{202}Hg$ X 0.252)

222     $\Delta^{200}Hg$ (‰) = $\delta^{200}Hg$ – ($\delta^{202}Hg$ X 0.502)

223     $\Delta^{201}Hg$ (‰) = $\delta^{201}Hg$ – ($\delta^{202}Hg$ X 0.752)

224   Total Hg in the diluted digest mixtures was monitored by MC-ICP-MS using ^{202}Hg signals:

225   mean recoveries of 95 ± 6% (n = 72) for samples and 93 ± 12% (n =10) for certified reference

226   materials were found, ensuring efficient digestion of samples. Hg levels in blanks were below

227   the detection limit. Reproducibility of Hg isotope measurements was assessed by analyzing

228   UM-Almadén (n = 13), ETH-Fluka (n = 12) and the biological tissue procedural standards NRC

229   TORT-3, ERM-BCR-464, and IAEA-436 (n = 10) (SI Table S1). Only one analysis was performed

230   per sample, but measured isotope signatures as well as analytical reproducibility of

231   standards were found to be in agreement with previously published values (Blum et al.,

232   2013; Jiskra et al., 2017; M. Li et al., 2016; Masbou et al., 2013).

233   **2.5 Statistics**

234   Data was first checked for normality (Shapiro–Wilks test) and homogeneity of

235   variances (Bartlett test). When these conditions were met, one-way ANOVAs were

236   performed to test for differences between groups, followed by Tukey's HSD tests when more

237   than two groups were compared. Otherwise, non-parametric analogues were used, i.e.

238   Kruskal–Wallis tests (KW), followed by Conover–Iman multiple comparison tests with

239   Bonferroni's adjustment in the presence of several groups.

240   Depending on data distribution (Shapiro–Wilks test), Pearson or Spearman correlation tests

241   were used to investigate the correlation between shark THg concentration and other

242   variables (length, mass, $\delta^{15}N$ and $\delta^{13}C$).

243   Using $\delta^{13}C$ and $\delta^{15}N$ values, standard ellipse areas encompassing 95% of the data (SEA$_B$,

244   Bayesian SEA) were used to quantify the niche width and overlap between the two shark

245   species, using the "SIBER" package (Jackson et al., 2011). The SEA$_B$ constitutes a proxy of the

246   feeding niche occupied by one species while the overlap between SEA$_B$ quantifies the trophic

247 competition between species. The SEA_B overlap is expressed as a proportion of the non-

248 overlapping area of the two ellipses.

249 Linear regressions were used to assess the relationships between i) Hg metabolism (using

250 $\delta^{202}Hg$ as a proxy for MeHg demethylation) and shark age (using length as a proxy for age)

251 (Bolea-Fernandez et al., 2019), ii) Hg MIF ($\Delta^{199}Hg$) and Hg MIF ($\Delta^{201}Hg$) as an indicator of

252 MeHg photodemethylation *versus* iHg photoreduction in seawater (Bergquist and Blum,

253 2007), iii) Hg MIF ($\Delta^{199}Hg$) and Hg MDF ($\delta^{202}Hg$) as an indicator of Hg photodegradation

254 *versus* microbial transformation (Bergquist and Blum, 2007).

255 Mean values are expressed with one standard deviation (1SD) unless otherwise stated (2SD).

256 All statistical analyses were performed using the open source software R (version 3.6.1, R

257 Core Team, 2019).

258

3. Results

259

3.1 Comparison of the two shark species

260

261   Tiger sharks had higher length (ANOVA; $p < 0.001$) but similar body mass (KW; $p >$

262 0.05) than bull shark (SI Table S2). The bull shark showed significantly higher THg

263 concentration (4148 ± 3069 ng·g^{-1}) (KW; $p < 0.01$), as well as higher muscle $\delta^{15}N$ ($14.22 \pm$

264 0.47 ‰) and $\delta^{13}C$ values (-16.00 ± 0.58 ‰) (ANOVA; $p < 0.001$) compared to the tiger shark

265 (3186 ± 1252 ng·g^{-1}, 13.27 ± 0.54 ‰, -17.01 ± 0.49 ‰ for THg, $\delta^{15}N$ and $\delta^{13}C$ values,

266 respectively) (SI Table S2). THg was positively correlated with total length and body mass for

267 both the bull (Pearson; $p < 0.001$) and the tiger shark (Spearman; $p < 0.05$). THg was not

268 correlated with $\delta^{15}N$ or $\delta^{13}C$ values for either species. The two shark species showed similar

269   carbon and nitrogen isotopic niche area: 5.23 ‰² for the bull shark and 4.19 ‰² for the tiger

270   shark (SEA$_B$ with 95% credible interval), and a small area overlap of 18%. (SI Figure S1).

271   Concerning Hg isotopes, muscle Δ^{199}Hg and Δ^{201}Hg values, as well as δ^{202}Hg values were

272   significantly higher in bull sharks than in tiger sharks (Δ^{199}Hg and Δ^{201}Hg: ANOVA, $p < 0.001$;

273   δ^{202}Hg: KW, $p < 0.001$) (SI Table S2). No difference was found between species for Δ^{200}Hg

274   (0.08 ‰ and 0.06 ‰ for bull and tiger sharks respectively; ANOVA, $p > 0.05$). The two sharks

275   showed similar variability in Δ^{199}Hg values (Bartlett test, $p > 0.05$) (Figure 2A), whereas bull

276   sharks displayed higher variability for δ^{202}Hg values (from 1.04 to 2.82 ‰) compared to tiger

277   sharks (from 0.74 to 1.7 ‰) (Bartlett test, $p < 0.001$) (Figure 2B). Δ^{199}Hg and δ^{202}Hg values

278   were not correlated with δ^{15}N or δ^{13}C values for either species ($p > 0.05$). Δ^{199}Hg values were

279   not correlated with body length in the two shark species ($p > 0.05$). A positive correlation

280   was found between length and δ^{202}Hg values for the two species ($p < 0.001$; $R^2=0.70$ for the

281   bull shark, and $R^2=0.31$ for the tiger shark) (Figures 3A and 3B), and between THg and δ^{202}Hg

282   only for the bull shark ($p < 0.001$, SI Figure S2). MeHg accounted for 95 ± 8% of THg in the

283   tiger shark and the MeHg fraction was not correlated with length nor δ^{202}Hg values (SI Figure

284   S3).

285   **3.2 Comparison between sharks and prey**

286   Δ^{199}Hg in prey species exhibited a wide range of values, from 1.94‰ in the

287   deepwater snapper to 2.72‰ in the lyretail grouper (SI Table S3 and Figure 2A). The bull

288   shark displayed similar Δ^{199}Hg as the yellowfin tuna and the giant trevally, while the tiger

289   shark shared similar Δ^{199}Hg with the deepwater snapper (ANOVA; $p > 0.05$) (Figure 2A). The

290   two shark species showed different Δ^{199}Hg values from all the other prey species (*i.e.* lyretail

291   grouper, wahoo, great barracuda, skipjack tuna, lantern fish) (ANOVA or KW; $p < 0.05$).

292   Muscle δ^{202}Hg in prey species ranged from 0.20‰ in the yellowfin tuna to 1.05‰ in the

293   great barracuda (SI Table S3). The bull shark showed significantly higher δ^{202}Hg than all the

294   prey species (ANOVA or KW; $p < 0.05$) (Figure 2B). δ^{202}Hg in the tiger shark was also higher

295   than in most of the prey species (ANOVA; $p < 0.001$) except for the lyretail grouper and the

296   great barracuda (ANOVA; $p < 0.05$).

297   **3.3 Hg sources**

298   The linear regression between Δ^{199}Hg and Δ^{201}Hg for the overall fish and shark

299   samples displayed a slope of 1.23 ± 0.05 ($R^2 = 0.87$, $p < 0.001$) (SI Figure S4) while the linear

300   regression between Δ^{199}Hg and δ^{202}Hg for teleost fish only displayed a slope of 0.64 ± 0.18

301   ($R^2 = 0.28$, $p < 0.01$) (SI Figure S5). The mesopelagic offshore lantern fish displayed similar

302   Δ^{199}Hg and δ^{202}Hg values than the giant trevally, as well as similar Δ^{199}Hg but higher δ^{202}Hg

303   than the deepwater snapper (SI Table S3). Compared to the previous study of Sackett *et al.*,

304   2017 in Hawaii (Sackett et al., 2017), significant higher δ^{202}Hg was found in the deepwater

305   snapper in the present study (ANOVA, $p < 0.05$) (SI Table S4). Despite no significant

306   difference in δ^{202}Hg and Δ^{199}Hg for the giant trevally between our study and Sackett *et al.*,

307   2017 (KW, $p > 0.05$), our values showed lower variance for both δ^{202}Hg and Δ^{199}Hg (Bartlett

308   test, $p < 0.05$).

309

310   **4. Discussion**

311   **4.1 Hg isotopes as tracers of shark ecology**

312   **- Foraging depth**

15

313   According to the previously documented decrease in Δ^{199}Hg values with depth (Blum

314   et al., 2013), the higher Δ^{199}Hg found in bull sharks is likely reflecting the use of shallower

315   waters as main feeding habitat compared to tiger sharks, which would forage in deeper

316   waters (Figure 2A). In previous studies in coastal environments, estuarine fish were

317   characterized either by higher (M. Li et al., 2016) or lower MIF signature (Senn et al., 2010)

318   than open ocean fish, depending on light penetration as a function of water turbidity. Except

319   during episodes of heavy rain, the water clarity in the coastal ecosystem of La Réunion Island

320   implies that Δ^{199}Hg values may possibly vary more over a vertical gradient (i.e. depending on

321   depth) than a horizontal gradient (i.e. depending on the distance to the shore). This

322   hypothesis is supported by the fact that epipelagic fish (i.e. living in the upper part of the

323   water column) from the inshore (e.g. wahoo and great barracuda) and offshore habitat (e.g.

324   skipjack and yellowfin tunas) did not differ in Δ^{199}Hg values (SI Table S3). Here, Δ^{199}Hg values

325   fully corroborate what was previously observed by telemetry studies at this site, showing a

326   higher presence of bull sharks in the coastal environment of La Réunion Island compared to

327   tiger sharks (Blaison et al., 2015). Similarly, bull sharks showed a preferential use of shallow

328   waters in the Indian Ocean when not migrating (usually less than 50 m with deepest dive at

329   164 m) (J. S. E. Lea et al., 2015), while tiger sharks have been recorded in oceanic waters

330   down to more than 1000 m (Afonso and Hazin, 2015).

331   **- Diet composition**

332   Numerous studies have confirmed that Δ^{199}Hg values are conserved between prey

333   and predators due to the absence of photochemical Hg MIF during trophic interactions or

334   metabolic processes (Kwon et al., 2016, 2012; Masbou et al., 2018), which makes this tool a

335   trophic tracer of major interest. At La Réunion Island, teleost fish species represent the large

336   majority of the prey consumed by both bull and tiger sharks, based on stomach contents (i.e.

337   respectively 93% and 78% in terms of mass percentage) (Trystram et al., 2016). Carangid

338   species such as the giant trevally constitute the most consumed family by bull sharks with

339   more than 40% of the ingested mass, while tiger sharks are more generalist predators and

340   target a large number of teleost families. Stable isotope tracers were in accordance with

341   stomach contents, as the bull shark had similar Δ^{199}Hg values (Figure 2A) but higher δ^{15}N

342   values (as a proxy for trophic position) than the giant trevally (δ^{15}N = 14.22 ‰ and 12.53 ‰

343   for bull sharks and giant trevally respectively; ANOVA, p < 0.001), supporting the idea that

344   carangid species are common prey for bull sharks. Alternatively, the largest giant trevallies

345   could also share the feeding habitat of bull sharks leading to competition for resources and

346   similar Δ^{199}Hg values. Associations between the two species have indeed been observed by

347   video and acoustic (Loiseau, unpublished data). On the other hand, taking into account that

348   epipelagic fish from the inshore and offshore habitats did not differ in MIF values (SI Table

349   S3), the Δ^{199}Hg overlap between the bull shark and yellowfin tuna may only reflect the use of

350   the same water depth across different food webs (i.e. respectively inshore and offshore)

351   rather than trophic interactions, since tuna species were not identified among bull shark

352   prey at La Réunion Island (Trystram et al., 2016). This underlines the importance of

353   considering the information given by stomach contents and trophic positions to interpret

354   Δ^{199}Hg values, which are preserved throughout food webs. Here, the tiger shark and the

355   deepwater snapper shared the same Δ^{199}Hg (Figure 2A) but different trophic positions (i.e.

356   higher δ^{15}N for the tiger shark; ANOVA, p < 0.001). As this bottom-associated snapper is

357   found in waters around 300 m depth (Trystram et al., 2015), it suggests that tiger sharks are

358   primarily targeting prey on the island slope. The two different isotopic approaches used in

359   this study (i.e. Δ^{199}Hg and δ^{15}N/δ^{13}C) both lead to the conclusion that the two shark species

17

360 occupy different trophic niches (different Δ^{199}Hg and small SEA$_b$ overlap) (Figure 2A and S2)

361 but also that their trophic niches are similar in size (similar variance for Δ^{199}Hg (Bartlett Test,

362 $p < 0.05$) and similar SEA$_b$). In a previous study based on δ^{13}C and δ^{15}N values, a trophic

363 independence of the epipelagic fish community (including both the bull and the tiger shark)

364 and the mesopelagic fish community was observed (Trystram et al., 2015). Here, Hg isotopes

365 confirm segregation between bull sharks and deep species such as the deepwater snapper,

366 but in contrast, provide evidence that tiger sharks rely on mesopelagic resources.

367 Overall, these results highlight the interest of Hg isotopes to address fundamental ecological

368 questions, such as habitat use and trophic energy transfers (Tsui et al., 2020).

4.2 Hg isotopes as tracers of shark metabolism

369

370 **- Comparison between sharks and bony fish**

371 While Δ^{199}Hg values in sharks were comparable to those of other fish species in this

372 area (Figure 2A), δ^{202}Hg values were generally higher in sharks compared to their potential

373 teleost prey (Figure 2B). More precisely, both shark species stand out from their prey by

374 more than 1 ‰ in δ^{202}Hg while having similar Δ^{199}Hg values. To our knowledge, such high

375 δ^{202}Hg values (i.e. 1.9 ‰ in the bull shark and 1.2 ‰ in the tiger shark) have never been

376 reported in fish. However, similar high values have been documented in mammals, including

377 humans, that are able to metabolize MeHg to inorganic Hg by demethylation in the liver

378 (Laffont et al., 2011; Masbou et al., 2018, 2015; Perrot et al., 2016). The preferential

379 demethylation of light Hg isotopes induces an increase in δ^{202}Hg in the remaining MeHg pool

380 that is ultimately accumulated in other tissues such as muscle (Perrot et al., 2016). This

381 increase in MeHg δ^{202}Hg following demethylation varies from about 0.3 ‰ in terrestrial

382 mammals (Ma et al., 2018; Masbou et al., 2018), to around 1 ‰ in aquatic mammals (Perrot

383 et al., 2016, 2012) and around 2 ‰ in humans (Laffont et al., 2011, 2009). Previous studies

384 on mercury speciation have concluded that MeHg demethylation can occur in fish liver and

385 intestine (Gonzalez et al., 2005; Wang et al., 2017). However, experimental studies using Hg

386 isotopes in fish muscle do not allow to draw clear conclusions, with either no change in MDF

387 signature between Hg trophic source and consumer (Feng et al., 2015; Kwon et al., 2012), or

388 a positive (+ 0.35 ‰) (Kwon et al., 2013) or a negative shift in δ^{202}Hg values (- 0.19 ‰) (Kwon

389 et al., 2016). In our study, δ^{202}Hg values in sharks were well above fractionation values

390 previously published in fish (e.g. + 1.4 ‰ between the bull shark and the giant trevally), with

391 the bull shark having higher δ^{202}Hg than all teleost species analyzed. This study represents

392 the first isotopic investigation of Hg metabolism in sharks and supports the existence of

393 MeHg demethylation in these predators.

394   High THg concentrations (around 150 µg·L^{-1}) were found in the blood plasma of South

395 African white sharks *Carcharodon carcharias*, at levels considered as toxic in other

396 vertebrates (Merly et al., 2019). Despite this contamination, no alteration of the body

397 condition nor negative effects on health parameters were observed suggesting that sharks

398 may have protective mechanisms that mitigate Hg toxicity. Demethylation in sharks could

399 therefore represent a mechanism limiting the accumulation of MeHg and its toxic effects.

400 Moreover, MeHg concentrations are generally much higher in muscle compared to other

401 organs such liver, kidney and brain in shark species (Bergés-Tiznado et al., 2015; Nam et al.,

402 2011), suggesting that muscle could represent a storage tissue less sensitive to MeHg toxicity

403 in sharks.

404   **- Hg metabolism over age**

19

405   δ^{202}Hg values increased with length, a proxy for age, in the two shark species studied

406   here (Figures 3A and 3B). Most of the sharks were sub-adults and adults, and larger than the

407   size at which the ontogenetic change in habitat and diet occurs (Habegger et al., 2012; Lowe

408   et al., 1996). Furthermore, in the two shark species, none of the trophic markers analyzed

409   (δ^{13}C, δ^{15}N, Δ^{199}Hg) were correlated with size. δ^{13}C and δ^{15}N were also not correlated with

410   δ^{202}Hg, which does not support the influence of ontogenetic diet changes on δ^{202}Hg values.

411   On the other hand, an enhancement of the demethylation rate with age was recently

412   identified in the long-finned pilot whale *Globicephala melas*, leading to the decrease of the

413   MeHg fraction in the muscle of older whales (from 99% to 65%) (Bolea-Fernandez et al.,

414   2019). Since MeHg has higher δ^{202}Hg values compared to inorganic Hg (iHg) (Perrot et al.,

415   2016), the decrease in MeHg fraction alongside the increase in iHg fraction in pilot whales

416   was accompanied by a drop in δ^{202}Hg values (around 1 ‰ decrease) (Bolea-Fernandez et al.,

417   2019). In our bull shark samples, MeHg accounted for 95% of total Hg, which is consistent

418   with previous studies on this species (Matulik et al., 2017) or on other sharks (de Carvalho et

419   al., 2014; Nam et al., 2011; Pethybridge et al., 2010). Moreover, no correlation was found

420   between MeHg fraction and δ^{202}Hg or shark length (SI Figure S3A and S3B). These results

421   imply that the change in δ^{202}Hg with age in shark muscle is unlikely to be the result of a

422   variation in Hg speciation (i.e. MeHg versus iHg fraction). We thus hypothesize that the

423   increase in δ^{202}Hg values with length could reflect a higher extent of MeHg demethylation in

424   the liver of older sharks, before preferential storage of the remaining MeHg over iHg in

425   muscle. By contrast, the aging muscle in pilot whale may gradually favor the storage of iHg

426   over MeHg (Bolea-Fernandez et al., 2019). Moreover, a positive correlation was also

427   observed between the δ^{202}Hg values and THg (as a proxy for MeHg) concentration only in

428   the bull shark muscle (SI Figure S2). Such a positive correlation between δ^{202}Hg and THg was

429 previously observed in teleost fish species and were attributed to the excretion of

430 isotopically light Hg by fish during Hg bioaccumulation (Bergquist and Blum, 2007). In the

431 present study, the shift in Hg MDF signatures between sharks and their prey (e.g. + 1.4 ‰ for

432 δ^{202}Hg between the bull shark and the giant trevally) is well above the values attributed

433 experimentally to excretion in teleost fish (e.g. + 0.35 ‰ between the amberjack *Seriola*

434 *dumerili* compared to its food) (Kwon et al., 2013). However, preferential efflux of MeHg

435 with light Hg isotopes over time, through urinary or biliary excretion (Le Croizier et al.,

436 2019a, 2018), may also contribute to the increase in δ^{202}Hg values observed in shark muscle.

437 In addition, as previously proposed in pilot whales (Bolea-Fernández et al., 2019), it is

438 possible that muscle MeHg can be recycled to the liver and undergo additional

439 demethylation. Thus, older sharks may have experienced more MeHg exchanges between

440 liver and muscle, leading to higher δ^{202}Hg values in the remaining MeHg. This hypothesis

441 would explain the increase in δ^{202}Hg with shark length and THg concentration which both

442 increase with age, respectively due to growth and bioaccumulation.

443 According to length, the age of individual sharks is supposed to vary from around 5

444 years to more than 25 years for bull sharks (Natanson et al., 2014) and from around 2 years

445 to more than 15 years for tiger sharks (Meyer et al., 2014). As bull sharks are on average

446 older and display a broader year range between individuals, this could explain their higher

447 δ^{202}Hg values and higher intraspecific variability compared to tiger sharks (Figure 2B), caused

448 by an increase in demethylation and / or more liver-muscle exchanges over time.

449 **4.3 Hg exposure sources to sharks**

450 **- Hg cycle in the shark environment**

451   In open oceans, Hg inputs to the surface waters mainly occur through rainfall wet

452   deposition of inorganic Hg (iHg) and atmospheric dissolution of gaseous Hg (Hg(0)) (Zhang et

453   al., 2014). Although the processes responsible for the mass-independent fractionation of

454   even Hg isotopes remain uncertain, Δ^{200}Hg is thought to result from high-altitude Hg photo-

455   oxidation in the tropopause (Chen et al., 2012). iHg wet deposition is characterized by a

456   Δ^{200}Hg between 0 and 0.3 ‰ while Δ^{200}Hg of atmospheric Hg(0) ranges from -0.11 to -0.01

457   ‰ (Enrico et al., 2016; Gratz et al., 2010). In the present study, Δ^{200}Hg values were similar

458   between the two shark species (i.e. 0.08 ± 0.04 ‰ in the bull shark and 0.06 ± 0.04 ‰ in the

459   tiger shark) (SI Table S2), implying that the iHg precursor to MeHg in sharks originates from a

460   common source, which may correspond to a combination of rainfall iHg and gaseous Hg(0)

461   (with positive and negative Δ^{200}Hg values, respectively). Although to our knowledge there is

462   still no data on the isotopic signature of Hg(0) in this region, preliminary Δ^{200}Hg in rainwater

463   collected at La Réunion Island is 0.12 ‰ (Araujo et al., unpublished data), which suggests

464   that MeHg in sharks is mostly derived from the methylation of iHg from wet deposition to

465   the marine ecosystem, as previously observed in other aquatic ecosystems (Lepak et al.,

466   2018).

467   Under the action of solar radiation, dissolved MeHg will be transformed into iHg by

468   photodemethylation, while dissolved iHg will be transformed into Hg(0) by photoreduction.

469   Photodemethylation of MeHg is characterized by a Δ^{199}Hg/Δ^{201}Hg ratio of 1.36 while

470   photodegradation of inorganic Hg leads to a ratio of 1.0 (Bergquist and Blum, 2007). In the

471   present study, overall fish and shark values displayed a mean Δ^{199}Hg/Δ^{201}Hg ratio of 1.23

472   indicating the dominance of MeHg demethylation over iHg photoreduction. This ratio is

473 consistent with those previously reported in coastal and pelagic ecosystems of oceanic

474 islands such as Hawaii (Blum et al., 2013; Sackett et al., 2017).

475 Experimental studies have shown that Hg photochemical degradation leads to an

476 approximate $\Delta^{199}Hg/\delta^{202}Hg$ slope of 2.4 whereas microbial transformation (no MIF) is

477 characterized by a slope of 0 (Bergquist and Blum, 2007). In our study, the Hg isotopic

478 signatures of the teleost prey displayed a $\Delta^{199}Hg/\delta^{202}Hg$ slope of 0.64 (SI Figure S5),

479 indicating the dominance of microbial transformation (i.e. methylation and/or

480 demethylation) over photochemical degradation, which is similar to previous studies on

481 Hawaiian marine bottomfish (Sackett et al., 2017) and coastal marine fish from the Gulf of

482 Mexico (Senn et al., 2010).

483 **- Hg isotope signatures in shark prey**

484 The main trophic MeHg vector for the bull shark at La Réunion Island is thought to be

485 constituted by nearshore fish such as the giant trevally (Trystram et al., 2015) which shared

486 similar $\Delta^{199}Hg$ and $\delta^{202}Hg$ with offshore epipelagic species such as the skipjack tuna (SI Table

487 S3, Figure 4). This result would suggest that MeHg to which bull sharks are exposed via

488 trophic transfer originates from the offshore environment (Figure 4). This observation

489 contrasts with the findings of a previous study in Hawaii where terrestrial freshwater inputs

490 to coastal sediments were the primary MeHg source for the giant trevally (Sackett et al.,

491 2017), resulting in higher inter-individual variability for both $\Delta^{199}Hg$ and $\delta^{202}Hg$ compared to

492 our values (Bartlett test, $p < 0.05$; SI Table S4). This strengthens the hypothesis of a limited

493 input of MeHg by freshwater runoff of estuarine waters into the coastal ecosystem of La

494 Réunion Island. Rather, MeHg around La Reunion originates from methylation of iHg that is

495 supplied by rainwater to the marine environment, as suggested by $\Delta^{200}Hg$ values.

496   According to Δ^{199}Hg values, mesopelagic species such as the deepwater snapper

497   constitute the main vector of Hg trophic contamination for tiger sharks (Figure 2A). The

498   deepwater snapper only shared similar Δ^{199}Hg with the lantern fish (SI Table S3, Figure 4).

499   This is in full agreement with stomach content observations, which revealed that

500   mesopelagic teleosts and especially lantern fish are the major prey of the deepwater

501   snapper, accounting for around 60% of the total prey abundance (Trystram, 2016). In Hawaii,

502   Hg isotopic signatures of bottom fish including deepwater snappers revealed the

503   incorporation of mesopelagic offshore MeHg sources into the slope sediments, where MeHg

504   was subject to additional negative MDF (due to microbial methylation and/or

505   demethylation) before transfer to the marine consumers (Sackett et al., 2017). Here, a lower

506   δ^{202}Hg was similarly found in the deepwater snapper compared to the lantern fish (SI Table

507   S3, Figure 4). We thus suggest that the decrease in δ^{202}Hg between the mesopelagic source

508   and the deepwater snapper is related to its partial consumption of benthic prey (around 20%

509   of the total prey abundance) (Trystram, 2016) and consequent exposure to a MeHg pool

510   having undergone microbial MDF (i.e. methylation and/or demethylation) in sediments

511   (Figure 4). The consumption of benthic prey could also have exposed the deepwater snapper

512   to another source of MeHg produced in the sediments and characterized by a lower δ^{202}Hg

513   values than mesopelagic MeHg.

514   As previously observed for marine fish species in the central Pacific (Blum et al., 2013;

515   Sackett et al., 2017), both bull and tiger sharks were exposed to two different MeHg pools

516   derived from the same main source of oceanic origin, produced from deposited atmospheric

517   iHg. The bull shark was exposed to epipelagic offshore MeHg, which was dietary transferred

518   to the epipelagic nearshore habitat (Figure 4). On the other hand, the tiger shark was

519 exposed to a mixed pool of (i) mesopelagic offshore MeHg and (ii) benthic MeHg subject to

520 bacterial transformation in sediments.

521

5. Conclusion

523 Hg MIF signatures allowed to characterize the vertical feeding habitat of sharks, revealing

524 that bull sharks forage in shallow water while tiger sharks use deeper habitat on the island

525 slope. Our study highlights the potential of Δ^{199}Hg values for tracing the ecology of marine

526 species and brings important new perspectives on the habitat use of coastal predators in a

527 context of increasing human-shark interactions. Using Hg MDF signatures, our results also

528 revealed for the first time the capacity of sharks to breakdown MeHg via demethylation. This

529 may limit MeHg concentrations in these vulnerable species, among the most contaminated

530 in the animal kingdom.

531

544

REFERENCES

Afonso, A.S., Hazin, F.H.V., 2015. Vertical Movement Patterns and Ontogenetic Niche Expansion in the Tiger Shark, Galeocerdo cuvier. PLOS ONE 10, e0116720. https://doi.org/10.1371/journal.pone.0116720

Baum, J.K., Myers, R.A., Kehler, D.G., Worm, B., Harley, S.J., Doherty, P.A., 2003. Collapse and Conservation of Shark Populations in the Northwest Atlantic. Science 299, 389–392. https://doi.org/10.1126/science.1079777

Bergquist, B.A., Blum, J.D., 2007. Mass-Dependent and -Independent Fractionation of Hg Isotopes by Photoreduction in Aquatic Systems. Science 318, 417–420. https://doi.org/10.1126/science.1148050

Bird, C.S., Veríssimo, A., Magozzi, S., Abrantes, K.G., Aguilar, A., Al-Reasi, H., Barnett, A., Bethea, D.M., Biais, G., Borrell, A., Bouchoucha, M., Boyle, M., Brooks, E.J., Brunnschweiler, J., Bustamante, P., Carlisle, A., Catarino, D., Caut, S., Cherel, Y., Chouvelon, T., Churchill, D., Ciancio, J., Claes, J., Colaço, A., Courtney, D.L., Cresson, P., Daly, R., Necker, L. de, Endo, T., Figueiredo, I., Frisch, A.J., Hansen, J.H., Heithaus, M., Hussey, N.E., Iitembu, J., Juanes, F., Kinney, M.J., Kiszka, J.J., Klarian, S.A., Kopp, D., Leaf, R., Li, Y., Lorrain, A., Madigan, D.J., Maljković, A., Malpica-Cruz, L., Matich, P., Meekan, M.G., Ménard, F., Menezes, G.M., Munroe, S.E.M., Newman, M.C., Papastamatiou, Y.P., Pethybridge, H., Plumlee, J.D., Polo-Silva, C., Quaeck-Davies, K., Raoult, V., Reum, J., Torres-Rojas, Y.E., Shiffman, D.S., Shipley, O.N., Speed, C.W., Staudinger, M.D., Teffer, A.K., Tilley, A., Valls, M., Vaudo, J.J., Wai, T.-C., Wells, R.J.D., Wyatt, A.S.J., Yool, A., Trueman, C.N., 2018. A global perspective on the trophic geography of sharks. Nature Ecology & Evolution 2, 299–305. https://doi.org/10.1038/s41559-017-0432-z

Blaison, A., Jaquemet, S., Guyomard, D., Vangrevelynghe, G., Gazzo, T., Cliff, G., Cotel, P., Soria, M., 2015. Seasonal variability of bull and tiger shark presence on the west coast of Reunion Island, western Indian Ocean. African Journal of Marine Science 37, 199–208. https://doi.org/10.2989/1814232X.2015.1050453

Blum, J.D., Popp, B.N., Drazen, J.C., Anela Choy, C., Johnson, M.W., 2013. Methylmercury production below the mixed layer in the North Pacific Ocean. Nature Geosci 6, 879–884. https://doi.org/10.1038/ngeo1918

Bodin, N., Lesperance, D., Albert, R., Hollanda, S., Michaud, P., Degroote, M., Churlaud, C., Bustamante, P., 2017. Trace elements in oceanic pelagic communities in the western Indian Ocean. Chemosphere 174, 354–362. https://doi.org/10.1016/j.chemosphere.2017.01.099

Bolea-Fernández, E., Rua-Ibarz, A., Krupp, E., Feldmann, J., Vanhaecke, F., 2019. High-precision isotopic analysis sheds new light on mercury metabolism in long-finned pilot whales (Globicephala melas). Scientific Reports 9. https://doi.org/10.1038/s41598-019-43825-z

Bolea-Fernandez, E., Rua-Ibarz, A., Krupp, E.M., Feldmann, J., Vanhaecke, F., 2019. High-precision isotopic analysis sheds new light on mercury metabolism in long-finned pilot whales (Globicephala melas). Scientific Reports 9, 7262. https://doi.org/10.1038/s41598-019-43825-z

Bosch, A.C., O'Neill, B., Sigge, G.O., Kerwath, S.E., Hoffman, L.C., 2016. Heavy metal accumulation and toxicity in smoothhound (Mustelus mustelus) shark from Langebaan Lagoon, South Africa. Food Chemistry 190, 871–878. https://doi.org/10.1016/j.foodchem.2015.06.034

Cáceres-Saez, I., Haro, D., Blank, O., Aguayo Lobo, A., Dougnac, C., Arredondo, C., Cappozzo, H.L., Guevara, S.R., 2018. High status of mercury and selenium in false killer whales (Pseudorca crassidens, Owen 1846) stranded on Southern South America: A possible toxicological concern? Chemosphere 199, 637–646. https://doi.org/10.1016/j.chemosphere.2018.02.046

592 Chen, J., Hintelmann, H., Feng, X., Dimock, B., 2012. Unusual fractionation of both odd and even
593   mercury isotopes in precipitation from Peterborough, ON, Canada. Geochimica et
594   Cosmochimica Acta 90, 33–46. https://doi.org/10.1016/j.gca.2012.05.005

595 de Carvalho, G.G.A., Degaspari, I.A.M., Branco, V., Canário, J., de Amorim, A.F., Kennedy, V.H.,
596   Ferreira, J.R., 2014. Assessment of Total and Organic Mercury Levels in Blue Sharks (Prionace
597   glauca) from the South and Southeastern Brazilian Coast. Biol Trace Elem Res 159, 128–134.
598   https://doi.org/10.1007/s12011-014-9995-6

599 Dicken, M.L., Hussey, N.E., Christiansen, H.M., Smale, M.J., Nkabi, N., Cliff, G., Wintner, S.P., 2017.
600   Diet and trophic ecology of the tiger shark (Galeocerdo cuvier) from South African waters.
601   PLOS ONE 12, e0177897. https://doi.org/10.1371/journal.pone.0177897

602 Emslie, M.J., Cheal, A.J., Logan, M., 2017. The distribution and abundance of reef-associated
603   predatory fishes on the Great Barrier Reef. Coral Reefs 36, 829–846.
604   https://doi.org/10.1007/s00338-017-1573-x

605 Enrico, M., Roux, G.L., Marusczak, N., Heimbürger, L.-E., Claustres, A., Fu, X., Sun, R., Sonke, J.E.,
606   2016. Atmospheric Mercury Transfer to Peat Bogs Dominated by Gaseous Elemental Mercury
607   Dry Deposition. Environ. Sci. Technol. 50, 2405–2412.
608   https://doi.org/10.1021/acs.est.5b06058

609 Espinoza, M., Heupel, M.R., Tobin, A.J., Simpfendorfer, C.A., 2016. Evidence of Partial Migration in a
610   Large Coastal Predator: Opportunistic Foraging and Reproduction as Key Drivers? PLOS ONE
611   11, e0147608. https://doi.org/10.1371/journal.pone.0147608

612 Feng, C., Pedrero, Z., Gentès, S., Barre, J., Renedo, M., Tessier, E., Berail, S., Maury-Brachet, R.,
613   Mesmer-Dudons, N., Baudrimont, M., Legeay, A., Maurice, L., Gonzalez, P., Amouroux, D.,
614   2015. Specific Pathways of Dietary Methylmercury and Inorganic Mercury Determined by
615   Mercury Speciation and Isotopic Composition in Zebrafish (Danio rerio). Environ. Sci. Technol.
616   49, 12984–12993. https://doi.org/10.1021/acs.est.5b03587

617 Ferretti, F., Myers, R.A., Serena, F., Lotze, H.K., 2008. Loss of Large Predatory Sharks from the
618   Mediterranean Sea. Conservation Biology 22, 952–964. https://doi.org/10.1111/j.1523-
619   1739.2008.00938.x

620 Gehrke, G.E., Blum, J.D., Slotton, D.G., Greenfield, B.K., 2011. Mercury Isotopes Link Mercury in San
621   Francisco Bay Forage Fish to Surface Sediments. Environ. Sci. Technol. 45, 1264–1270.
622   https://doi.org/10.1021/es103053y

623 Goix, S., Maurice, L., Laffont, L., Rinaldo, R., Lagane, C., Chmeleff, J., Menges, J., Heimbürger, L.-E.,
624   Maury-Brachet, R., Sonke, J.E., 2019. Quantifying the impacts of artisanal gold mining on a
625   tropical river system using mercury isotopes. Chemosphere 219, 684–694.
626   https://doi.org/10.1016/j.chemosphere.2018.12.036

627 Gonzalez, P., Dominique, Y., Massabuau, J.C., Boudou, A., Bourdineaud, J.P., 2005. Comparative
628   Effects of Dietary Methylmercury on Gene Expression in Liver, Skeletal Muscle, and Brain of
629   the Zebrafish (Danio rerio). Environ. Sci. Technol. 39, 3972–3980.
630   https://doi.org/10.1021/es0483490

631 Gratz, L.E., Keeler, G.J., Blum, J.D., Sherman, L.S., 2010. Isotopic Composition and Fractionation of
632   Mercury in Great Lakes Precipitation and Ambient Air. Environ. Sci. Technol. 44, 7764–7770.
633   https://doi.org/10.1021/es100383w

634 Habegger, M.L., Motta, P.J., Huber, D.R., Dean, M.N., 2012. Feeding biomechanics and theoretical
635   calculations of bite force in bull sharks (Carcharhinus leucas) during ontogeny. Zoology 115,
636   354–364. https://doi.org/10.1016/j.zool.2012.04.007

637 Hammerschlag, N., Williams, L., Fallows, M., Fallows, C., 2019. Disappearance of white sharks leads to
638   the novel emergence of an allopatric apex predator, the sevengill shark. Scientific Reports 9,
639   1908. https://doi.org/10.1038/s41598-018-37576-6

640 Jackson, A.L., Inger, R., Parnell, A.C., Bearhop, S., 2011. Comparing isotopic niche widths among and
641   within communities: SIBER – Stable Isotope Bayesian Ellipses in R. Journal of Animal Ecology
642   80, 595–602. https://doi.org/10.1111/j.1365-2656.2011.01806.x

643 Janssen, S.E., Schaefer, J.K., Barkay, T., Reinfelder, J.R., 2016. Fractionation of Mercury Stable
644   Isotopes during Microbial Methylmercury Production by Iron- and Sulfate-Reducing Bacteria.
645   Environ. Sci. Technol. 50, 8077–8083. https://doi.org/10.1021/acs.est.6b00854
646 Jiskra, M., G. Wiederhold, J., Skyllberg, U., Kronberg, R.-M., Kretzschmar, R., 2017. Source tracing of
647   natural organic matter bound mercury in boreal forest runoff with mercury stable isotopes.
648   Environmental Science: Processes & Impacts 19, 1235–1248.
649   https://doi.org/10.1039/C7EM00245A
650 Kim, S.L., del Rio, C.M., Casper, D., Koch, P.L., 2012. Isotopic incorporation rates for shark tissues
651   from a long-term captive feeding study. J. Exp. Biol. 215, 2495–2500.
652   https://doi.org/10.1242/jeb.070656
653 Kiszka, J.J., Aubail, A., Hussey, N.E., Heithaus, M.R., Caurant, F., Bustamante, P., 2015. Plasticity of
654   trophic interactions among sharks from the oceanic south-western Indian Ocean revealed by
655   stable isotope and mercury analyses. Deep Sea Research Part I: Oceanographic Research
656   Papers 96, 49–58. https://doi.org/10.1016/j.dsr.2014.11.006
657 Krey, A., Ostertag, S.K., Chan, H.M., 2015. Assessment of neurotoxic effects of mercury in beluga
658   whales (Delphinapterus leucas), ringed seals (Pusa hispida), and polar bears (Ursus
659   maritimus) from the Canadian Arctic. Science of The Total Environment, Special Issue:
660   Mercury in Canada's North 509–510, 237–247.
661   https://doi.org/10.1016/j.scitotenv.2014.05.134
662 Kwon, S.Y., Blum, J.D., Carvan, M.J., Basu, N., Head, J.A., Madenjian, C.P., David, S.R., 2012. Absence
663   of fractionation of mercury isotopes during trophic transfer of methylmercury to freshwater
664   fish in captivity. Environmental science & technology 46, 7527.
665   https://doi.org/10.1021/es300794q
666 Kwon, S.Y., Blum, J.D., Chirby, M.A., Chesney, E.J., 2013. Application of mercury isotopes for tracing
667   trophic transfer and internal distribution of mercury in marine fish feeding experiments.
668   Environ. Toxicol. Chem. 32, 2322–2330. https://doi.org/10.1002/etc.2313
669 Kwon, S.Y., Blum, J.D., Madigan, D.J., Block, B.A., Popp, B.N., 2016. Quantifying mercury isotope
670   dynamics in captive Pacific bluefin tuna (*Thunnus orientalis*). Elem Sci Anth 4.
671   https://doi.org/10.12952/journal.elementa.000088
672 Laffont, L., Sonke, J.E., Maurice, L., Hintelmann, H., Pouilly, M., Sánchez Bacarreza, Y., Perez, T.,
673   Behra, P., 2009. Anomalous Mercury Isotopic Compositions of Fish and Human Hair in the
674   Bolivian Amazon. Environ. Sci. Technol. 43, 8985–8990. https://doi.org/10.1021/es9019518
675 Laffont, L., Sonke, J.E., Maurice, L., Monrroy, S.L., Chincheros, J., Amouroux, D., Behra, P., 2011. Hg
676   Speciation and Stable Isotope Signatures in Human Hair As a Tracer for Dietary and
677   Occupational Exposure to Mercury. Environmental Science & Technology 45, 9910–9916.
678   https://doi.org/10.1021/es202353m
679 Le Bourg, B., Kiszka, J.J., Bustamante, P., Heithaus, M.R., Jaquemet, S., Humber, F., 2019. Effect of
680   body length, trophic position and habitat use on mercury concentrations of sharks from
681   contrasted ecosystems in the southwestern Indian Ocean. Environmental Research 169, 387–
682   395. https://doi.org/10.1016/j.envres.2018.11.024
683 Le Croizier, G., Lacroix, C., Artigaud, S., Le Floch, S., Munaron, J.-M., Raffray, J., Penicaud, V., Rouget,
684   M.-L., Laë, R., Tito De Morais, L., 2019a. Metal subcellular partitioning determines excretion
685   pathways and sensitivity to cadmium toxicity in two marine fish species. Chemosphere 217,
686   754–762. https://doi.org/10.1016/j.chemosphere.2018.10.212
687 Le Croizier, G., Lacroix, C., Artigaud, S., Le Floch, S., Raffray, J., Penicaud, V., Coquillé, V., Autier, J.,
688   Rouget, M.-L., Le Bayon, N., Laë, R., Tito De Morais, L., 2018. Significance of metallothioneins
689   in differential cadmium accumulation kinetics between two marine fish species.
690   Environmental Pollution 236, 462–476. https://doi.org/10.1016/j.envpol.2018.01.002
691 Le Croizier, G., Lorrain, A., Schaal, G., Ketchum, J., Hoyos-Padilla, M., Besnard, L., Jean-Marie-
692   Munaron, Le Loc'h, F., Point, D., 2020. Trophic resources and mercury exposure of two
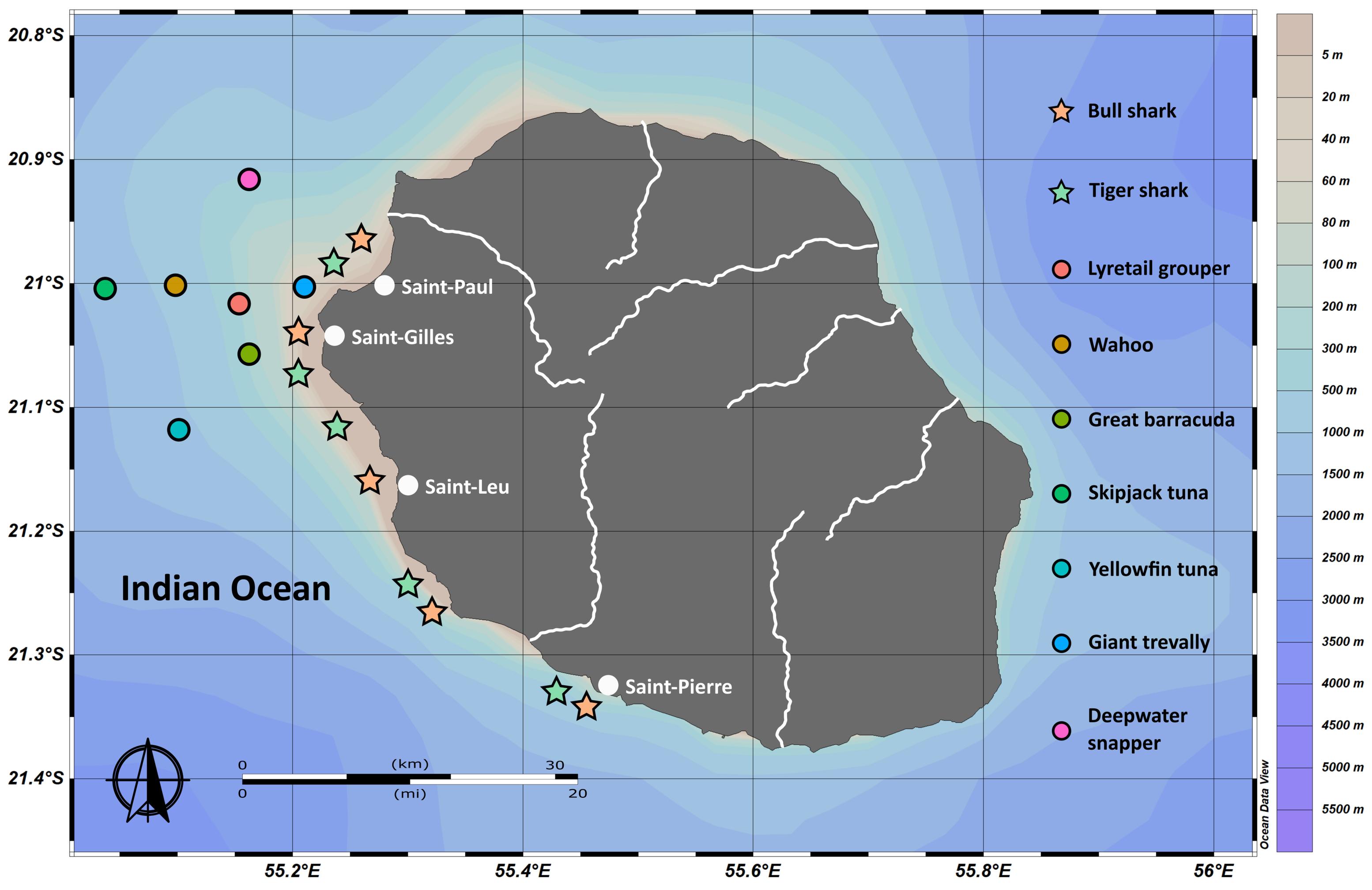
693   silvertip shark populations in the northeast Pacific Ocean. Chemosphere 126645.
694   https://doi.org/10.1016/j.chemosphere.2020.126645

695   Le Croizier, G., Schaal, G., Gallon, R., Fall, M., Le Grand, F., Munaron, J.-M., Rouget, M.-L., Machu, E.,
696   Le Loc'h, F., Laë, R., De Morais, L.T., 2016. Trophic ecology influence on metal
697   bioaccumulation in marine fish: Inference from stable isotope and fatty acid analyses.
698   Science of The Total Environment 573, 83–95.
699   https://doi.org/10.1016/j.scitotenv.2016.08.035

700   Le Croizier, G., Schaal, G., Point, D., Le Loc'h, F., Machu, E., Fall, M., Munaron, J.-M., Boyé, A., Walter,
701   P., Laë, R., Tito De Morais, L., 2019b. Stable isotope analyses revealed the influence of
702   foraging habitat on mercury accumulation in tropical coastal marine fish. Science of The Total
703   Environment 650, 2129–2140. https://doi.org/10.1016/j.scitotenv.2018.09.330

704   Lea, J. S. E., Humphries, N.E., Clarke, C.R., Sims, D.W., 2015. To Madagascar and back: long-distance,
705   return migration across open ocean by a pregnant female bull shark Carcharhinus leucas.
706   Journal of Fish Biology 87, 1313–1321. https://doi.org/10.1111/jfb.12805

707   Lea, James S. E., Wetherbee, B.M., Queiroz, N., Burnie, N., Aming, C., Sousa, L.L., Mucientes, G.R.,
708   Humphries, N.E., Harvey, G.M., Sims, D.W., Shivji, M.S., 2015. Repeated, long-distance
709   migrations by a philopatric predator targeting highly contrasting ecosystems. Scientific
710   Reports 5, 11202. https://doi.org/10.1038/srep11202

711   Lepak, R.F., Janssen, S.E., Yin, R., Krabbenhoft, D.P., Ogorek, J.M., DeWild, J.F., Tate, M.T., Holsen,
712   T.M., Hurley, J.P., 2018. Factors Affecting Mercury Stable Isotopic Distribution in Piscivorous
713   Fish of the Laurentian Great Lakes. Environ. Sci. Technol. 52, 2768–2776.
714   https://doi.org/10.1021/acs.est.7b06120

715   Li, M., Schartup, A.T., Valberg, A.P., Ewald, J.D., Krabbenhoft, D.P., Yin, R., Balcom, P.H., Sunderland,
716   E.M., 2016. Environmental Origins of Methylmercury Accumulated in Subarctic Estuarine Fish
717   Indicated by Mercury Stable Isotopes. Environ. Sci. Technol. 50, 11559–11568.
718   https://doi.org/10.1021/acs.est.6b03206

719   Li, M., Sherman, L.S., Blum, J.D., Grandjean, P., Mikkelsen, B., Weihe, P., Sunderland, E.M., Shine, J.P.,
720   2014. Assessing Sources of Human Methylmercury Exposure Using Stable Mercury Isotopes.
721   Environ. Sci. Technol. 48, 8800–8806. https://doi.org/10.1021/es500340r

722   Li, Y., Zhang, Y., Hussey, N.E., Dai, X., 2016. Urea and lipid extraction treatment effects on δ15N and
723   δ13C values in pelagic sharks. Rapid Communications in Mass Spectrometry 30, 1–8.
724   https://doi.org/10.1002/rcm.7396

725   Lowe, C.G., Wetherbee, B.M., Crow, G.L., Tester, A.L., 1996. Ontogenetic dietary shifts and feeding
726   behavior of the tiger shark, Galeocerdo cuvier, in Hawaiian waters. Environ Biol Fish 47, 203–
727   211. https://doi.org/10.1007/BF00005044

728   Ma, L., Evans, R.D., Wang, W., Georg, R.B., 2018. In vivo fractionation of mercury isotopes in tissues
729   of a mammalian carnivore (Neovison vison). Science of The Total Environment 627, 1228–
730   1233. https://doi.org/10.1016/j.scitotenv.2018.01.296

731   Madigan, D.J., Li, M., Yin, R., Baumann, H., Snodgrass, O.E., Dewar, H., Krabbenhoft, D.P., Baumann,
732   Z., Fisher, N.S., Balcom, P., Sunderland, E.M., 2018. Mercury Stable Isotopes Reveal Influence
733   of Foraging Depth on Mercury Concentrations and Growth in Pacific Bluefin Tuna. Environ.
734   Sci. Technol. 52, 6256–6264. https://doi.org/10.1021/acs.est.7b06429

735   Malpica-Cruz, L., Herzka, S.Z., Sosa-Nishizaki, O., Lazo, J.P., 2012. Tissue-specific isotope trophic
736   discrimination factors and turnover rates in a marine elasmobranch: empirical and modeling
737   results. Can. J. Fish. Aquat. Sci. 69, 551–564. https://doi.org/10.1139/f2011-172

738   Martin, U.M., Jaquemet, S., 2019. Effects of urea and lipid removal from Carcharhinus leucas and
739   Galeocerdo cuvier white muscle on carbon and nitrogen stable isotope ratios. Western
740   Indian Ocean Journal of Marine Science 18, 47-56–56.

741   Masbou, J., Point, D., Sonke, J.E., 2013. Application of a selective extraction method for
742   methylmercury compound specific stable isotope analysis (MeHg-CSIA) in biological
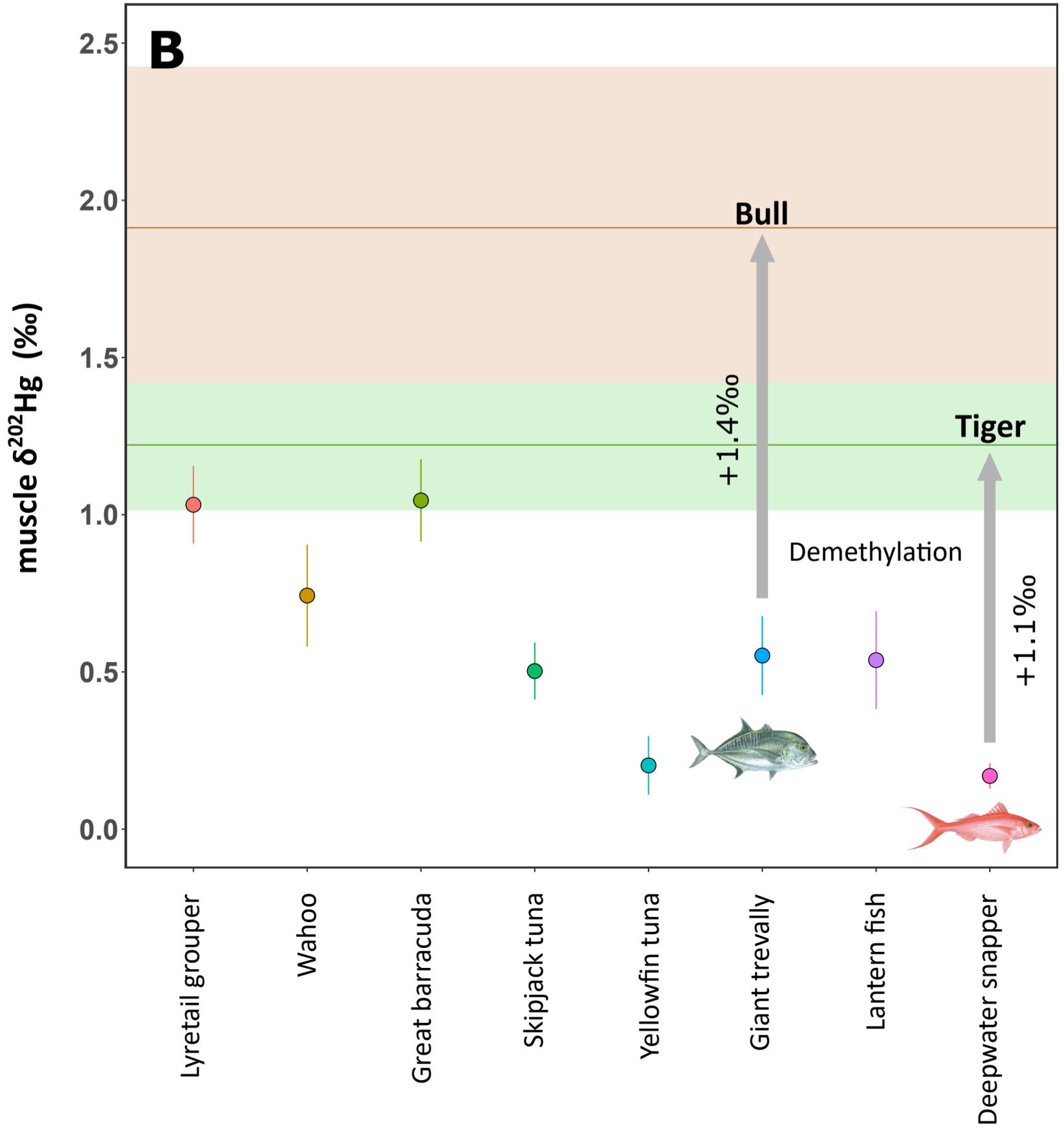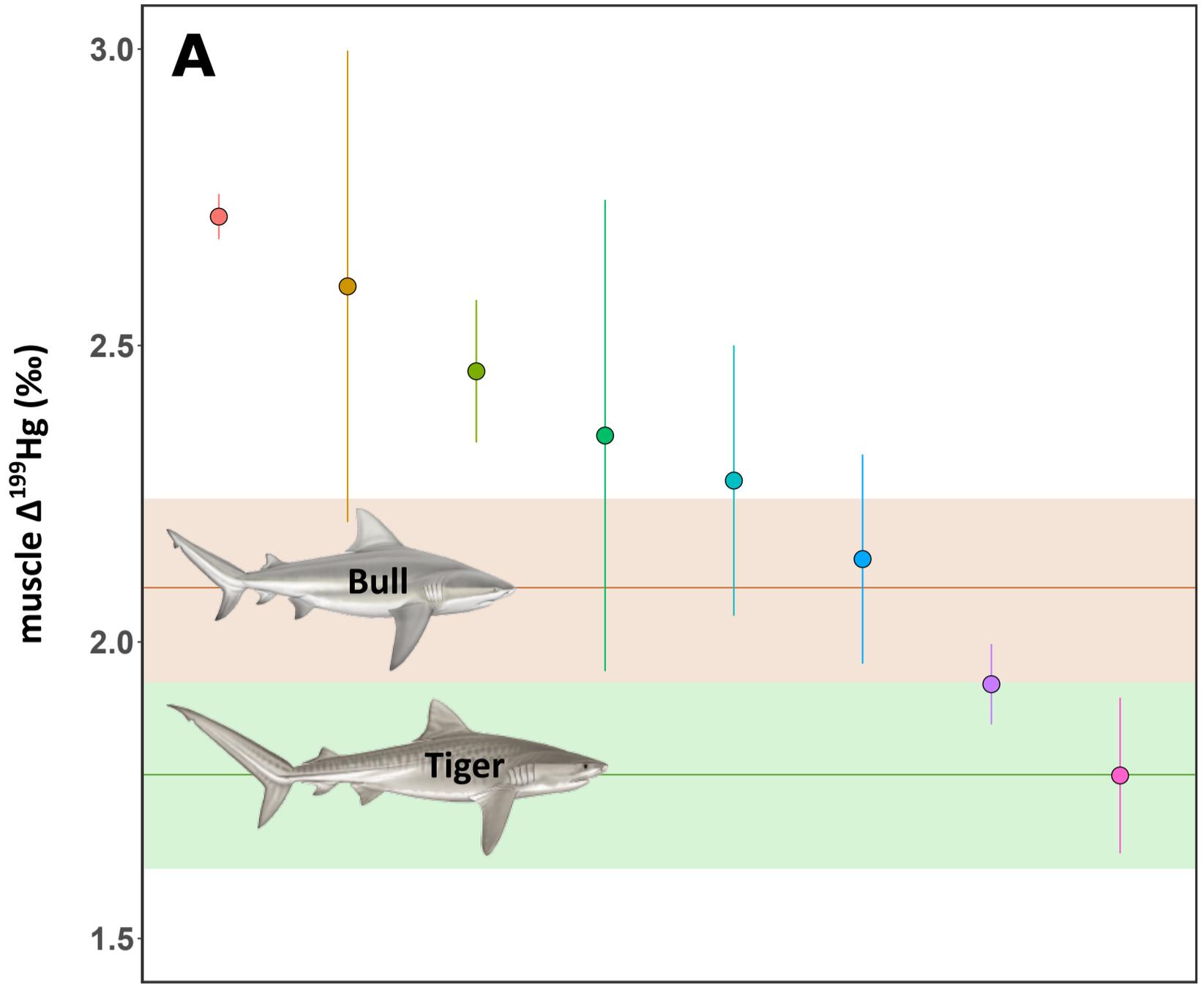743   materials. J. Anal. At. Spectrom. 28, 1620–1628. https://doi.org/10.1039/C3JA50185J

744 Masbou, J., Point, D., Sonke, J.E., Frappart, F., Perrot, V., Amouroux, D., Richard, P., Becker, P.R.,
745   2015. Hg Stable Isotope Time Trend in Ringed Seals Registers Decreasing Sea Ice Cover in the
746   Alaskan Arctic. Environ. Sci. Technol. 49, 8977–8985. https://doi.org/10.1021/es5048446
747 Masbou, J., Sonke, J.E., Amouroux, D., Guillou, G., Becker, P.R., Point, D., 2018. Hg-Stable Isotope
748   Variations in Marine Top Predators of the Western Arctic Ocean. ACS Earth Space Chem.
749   https://doi.org/10.1021/acsearthspacechem.8b00017
750 Matich, P., Heithaus, M.R., 2015. Individual variation in ontogenetic niche shifts in habitat use and
751   movement patterns of a large estuarine predator (Carcharhinus leucas). Oecologia 178, 347–
752   359. https://doi.org/10.1007/s00442-015-3253-2
753 Matulik, A.G., Kerstetter, D.W., Hammerschlag, N., Divoll, T., Hammerschmidt, C.R., Evers, D.C., 2017.
754   Bioaccumulation and biomagnification of mercury and methylmercury in four sympatric
755   coastal sharks in a protected subtropical lagoon. Marine Pollution Bulletin 116, 357–364.
756   https://doi.org/10.1016/j.marpolbul.2017.01.033
757 McKinney, M.A., Dean, K., Hussey, N.E., Cliff, G., Wintner, S.P., Dudley, S.F.J., Zungu, M.P., Fisk, A.T.,
758   2016. Global versus local causes and health implications of high mercury concentrations in
759   sharks from the east coast of South Africa. Science of The Total Environment 541, 176–183.
760   https://doi.org/10.1016/j.scitotenv.2015.09.074
761 Merly, L., Lange, L., Meÿer, M., Hewitt, A.M., Koen, P., Fischer, C., Muller, J., Schilack, V., Wentzel, M.,
762   Hammerschlag, N., 2019. Blood plasma levels of heavy metals and trace elements in white
763   sharks (Carcharodon carcharias) and potential health consequences. Marine Pollution
764   Bulletin 142, 85–92. https://doi.org/10.1016/j.marpolbul.2019.03.018
765 Meyer, C.G., Anderson, J.M., Coffey, D.M., Hutchinson, M.R., Royer, M.A., Holland, K.N., 2018.
766   Habitat geography around Hawaii's oceanic islands influences tiger shark (Galeocerdo cuvier
767   ) spatial behaviour and shark bite risk at ocean recreation sites. Scientific Reports 8, 4945.
768   https://doi.org/10.1038/s41598-018-23006-0
769 Meyer, C.G., O'Malley, J.M., Papastamatiou, Y.P., Dale, J.J., Hutchinson, M.R., Anderson, J.M., Royer,
770   M.A., Holland, K.N., 2014. Growth and Maximum Size of Tiger Sharks (Galeocerdo cuvier) in
771   Hawaii. PLoS ONE 9, e84799. https://doi.org/10.1371/journal.pone.0084799
772 Meyer, L., Pethybridge, H., Nichols, P.D., Beckmann, C., Bruce, B.D., Werry, J.M., Huveneers, C., 2017.
773   Assessing the Functional Limitations of Lipids and Fatty Acids for Diet Determination: The
774   Importance of Tissue Type, Quantity, and Quality. Front. Mar. Sci. 4.
775   https://doi.org/10.3389/fmars.2017.00369
776 Myers, R.A., Worm, B., 2003. Rapid worldwide depletion of predatory fish communities. Nature 423,
777   280–283. https://doi.org/10.1038/nature01610
778 Nam, D.-H., Adams, D.H., Reyier, E.A., Basu, N., 2011. Mercury and selenium levels in lemon sharks
779   (Negaprion brevirostris) in relation to a harmful red tide event. Environ Monit Assess 176,
780   549–559. https://doi.org/10.1007/s10661-010-1603-4
781 Natanson, L.J., Adams, D.H., Winton, M.V., Maurer, J.R., 2014. Age and Growth of the Bull Shark in
782   the Western North Atlantic Ocean. Transactions of the American Fisheries Society 143, 732–
783   743. https://doi.org/10.1080/00028487.2014.892537
784 Perrot, V., Masbou, J., V. Pastukhov, M., N. Epov, V., Point, D., Bérail, S., R. Becker, P., E. Sonke, J.,
785   Amouroux, D., 2016. Natural Hg isotopic composition of different Hg compounds in mammal
786   tissues as a proxy for in vivo breakdown of toxic methylmercury. Metallomics 8, 170–178.
787   https://doi.org/10.1039/C5MT00286A
788 Perrot, V., Pastukhov, M.V., Epov, V.N., Husted, S., Donard, O.F.X., Amouroux, D., 2012. Higher Mass-
789   Independent Isotope Fractionation of Methylmercury in the Pelagic Food Web of Lake Baikal
790   (Russia). Environ. Sci. Technol. 46, 5902–5911. https://doi.org/10.1021/es204572g
791 Pethybridge, H., Choy, C.A., Logan, J.M., Allain, V., Lorrain, A., Bodin, N., Somes, C.J., Young, J.,
792   Ménard, F., Langlais, C., Duffy, L., Hobday, A.J., Kuhnert, P., Fry, B., Menkes, C., Olson, R.J.,
793   2018. A global meta-analysis of marine predator nitrogen stable isotopes: Relationships
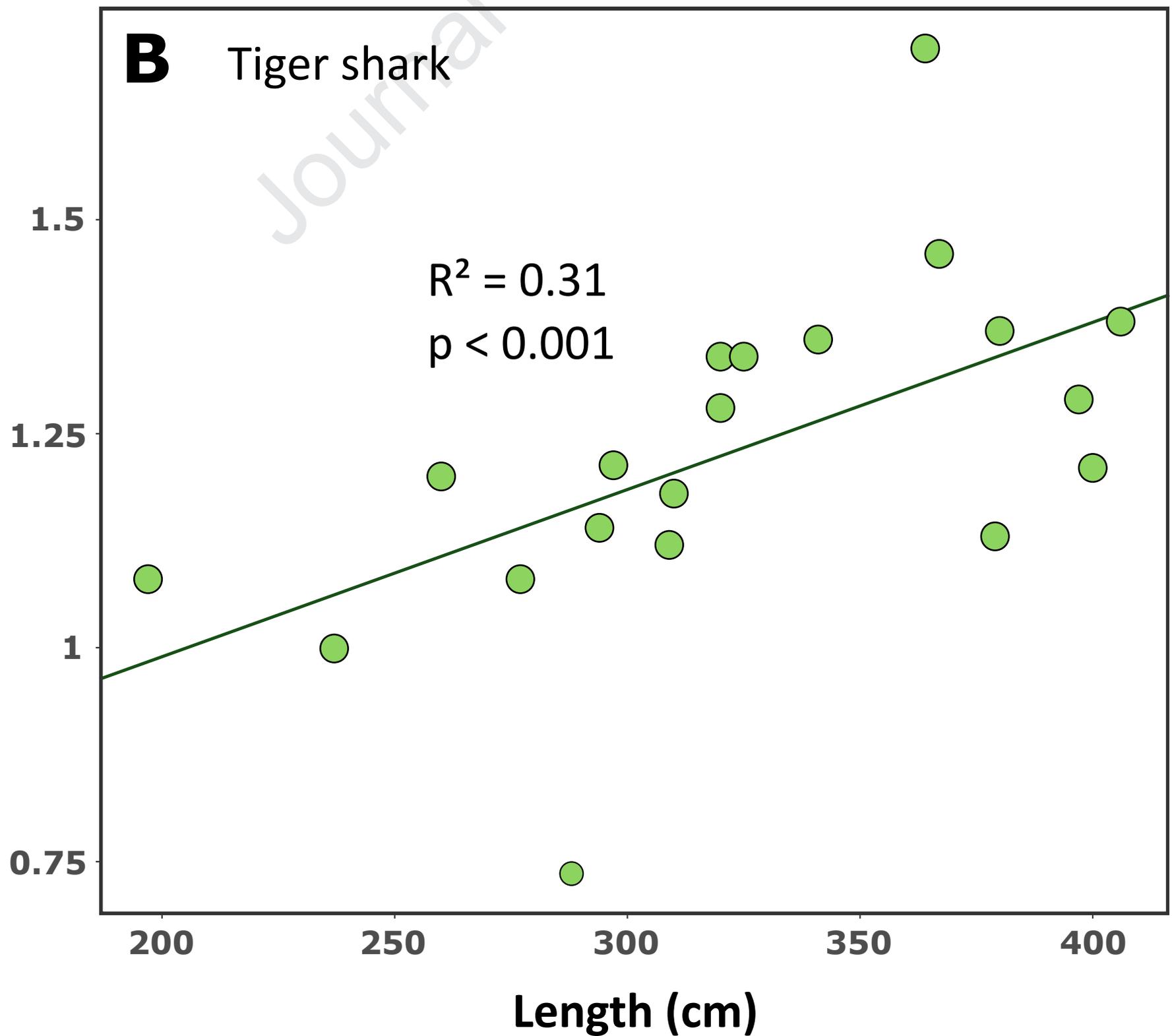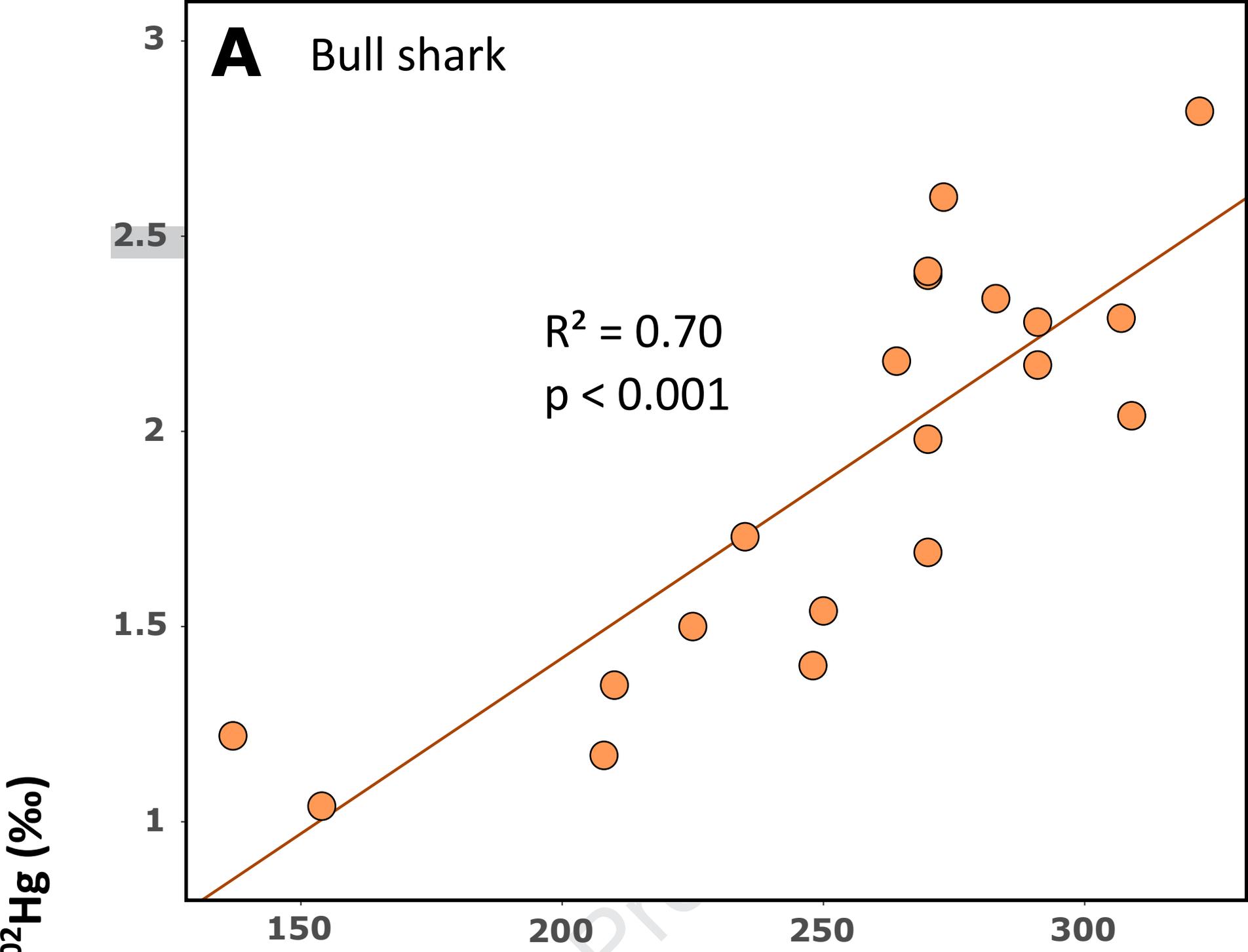
between trophic structure and environmental conditions. Global Ecology and Biogeography 27, 1043–1055. https://doi.org/10.1111/geb.12763

Pethybridge, H., Cossa, D., Butler, E.C.V., 2010. Mercury in 16 demersal sharks from southeast Australia: Biotic and abiotic sources of variation and consumer health implications. Marine Environmental Research 69, 18–26. https://doi.org/10.1016/j.marenvres.2009.07.006

Roff, G., Brown, C.J., Priest, M.A., Mumby, P.J., 2018. Decline of coastal apex shark populations over the past half century. Communications Biology 1, 223. https://doi.org/10.1038/s42003-018-0233-1

Roff, G., Doropoulos, C., Rogers, A., Bozec, Y.-M., Krueck, N.C., Aurellado, E., Priest, M., Birrell, C., Mumby, P.J., 2016. The Ecological Role of Sharks on Coral Reefs. Trends in Ecology & Evolution 31, 395–407. https://doi.org/10.1016/j.tree.2016.02.014

Ruiz-de-Cenzano, M., Rochina-Marco, A., Cervera, M.L., de la Guardia, M., 2014. Speciation of methylmercury in market seafood by thermal degradation, amalgamation and atomic absorption spectroscopy. Ecotoxicology and Environmental Safety 107, 90–96. https://doi.org/10.1016/j.ecoenv.2014.05.015

Sackett, D.K., Drazen, J.C., Choy, C.A., Popp, B., Pitz, G.L., 2015. Mercury Sources and Trophic Ecology for Hawaiian Bottomfish. Environ. Sci. Technol. 49, 6909–6918. https://doi.org/10.1021/acs.est.5b01009

Sackett, D.K., Drazen, J.C., Popp, B.N., Choy, C.A., Blum, J.D., Johnson, M.W., 2017. Carbon, Nitrogen, and Mercury Isotope Evidence for the Biogeochemical History of Mercury in Hawaiian Marine Bottomfish. Environ. Sci. Technol. 51, 13976–13984. https://doi.org/10.1021/acs.est.7b04893

Sardenne, F., Hollanda, S., Lawrence, S., Albert-Arrisol, R., Degroote, M., Bodin, N., 2017. Trophic structures in tropical marine ecosystems: a comparative investigation using three different ecological tracers. Ecological Indicators 81, 315–324. https://doi.org/10.1016/j.ecolind.2017.06.001

Scheuhammer, A., Braune, B., Chan, H.M., Frouin, H., Krey, A., Letcher, R., Loseto, L., Noël, M., Ostertag, S., Ross, P., Wayland, M., 2015. Recent progress on our understanding of the biological effects of mercury in fish and wildlife in the Canadian Arctic. Science of The Total Environment, Special Issue: Mercury in Canada's North 509–510, 91–103. https://doi.org/10.1016/j.scitotenv.2014.05.142

Senn, D.B., Chesney, E.J., Blum, J.D., Bank, M.S., Maage, A., Shine, J.P., 2010. Stable isotope (N, C, Hg) study of methylmercury sources and trophic transfer in the northern gulf of Mexico. Environ. Sci. Technol. 44, 1630–1637. https://doi.org/10.1021/es902361j

Trystram, C., 2016. Écologie trophique de poissons prédateurs et contribution à l'étude des réseaux trophiques marins aux abords de La Réunion.

Trystram, C., Rogers, K.M., Soria, M.M., Jaquemet, S., 2016. Feeding patterns of two sympatric shark predators in coastal ecosystems of an oceanic island. Canadian Journal of Fisheries and Aquatic Sciences. https://doi.org/10.1139/cjfas-2016-0105

Trystram, C., Roos, D., Guyomard, D., Jaquemet, S., 2015. Mechanisms of trophic partitioning within two fish communities associated with a tropical oceanic island. Western Indian Ocean Journal of Marine Science 14, 93–111.

Tsui, M.T.-K., Blum, J.D., Kwon, S.Y., 2020. Review of stable mercury isotopes in ecology and biogeochemistry. Science of The Total Environment 716, 135386. https://doi.org/10.1016/j.scitotenv.2019.135386

Wang, X., Wu, F., Wang, W.-X., 2017. In Vivo Mercury Demethylation in a Marine Fish (Acanthopagrus schlegeli). Environ. Sci. Technol. 51, 6441–6451. https://doi.org/10.1021/acs.est.7b00923

Werry, J.M., Lee, S.Y., Lemckert, C.J., Otway, N.M., 2012. Natural or Artificial? Habitat-Use by the Bull Shark, Carcharhinus leucas. PLOS ONE 7, e49796. https://doi.org/10.1371/journal.pone.0049796

845 Werry, J.M., Lee, S.Y., Otway, N.M., Hu, Y., Sumpton, W., 2011. A multi-faceted approach for
846   quantifying the estuarine–nearshore transition in the life cycle of the bull shark, Carcharhinus
847   leucas. Mar. Freshwater Res. 62, 1421–1431. https://doi.org/10.1071/MF11136

848 Werry, J.M., Planes, S., Berumen, M.L., Lee, K.A., Braun, C.D., Clua, E., 2014. Reef-Fidelity and
849   Migration of Tiger Sharks, Galeocerdo cuvier, across the Coral Sea. PLOS ONE 9, e83249.
850   https://doi.org/10.1371/journal.pone.0083249

851 Zhang, Y., Jaeglé, L., Thompson, L., 2014. Natural biogeochemical cycle of mercury in a global three-
852   dimensional ocean tracer model. Global Biogeochemical Cycles 28, 553–570.
853   https://doi.org/10.1002/2014GB004814

854 Zheng, W., Foucher, D., Hintelmann, H., 2007. Mercury isotope fractionation during volatilization of
855   Hg(0) from solution into the gas phase. Journal of Analytical Atomic Spectrometry 22, 1097–
856   1104. https://doi.org/10.1039/B705677J

857

⭐	Bull shark	
⭐	Tiger shark	
●	Lyretail grouper	
●	Wahoo	
●	Great barracuda	
●	Skipjack tuna	
●	Yellowfin tuna	
●	Giant trevally	
●	Deepwater snapper	

Indian Ocean

Saint-Paul
Saint-Gilles
Saint-Leu
Saint-Pierre

Ocean Data View

5 m
20 m
40 m
60 m
80 m
100 m
200 m
300 m
500 m
1000 m
1500 m
2000 m
2500 m
3000 m
3500 m
4000 m
4500 m
5000 m
5500 m

(km) 0   30
(mi) 0   20

20.8°S
20.9°S
21°S
21.1°S
21.2°S
21.3°S
21.4°S

55.2°E 55.4°E 55.6°E 55.8°E 56°E

Panel A: muscle Δ^{199}Hg (‰)

Panel B: muscle δ^{202}Hg (‰)

Bull

Tiger

+1.4‰

Demethylation

+1.1‰

Lyretail grouper, Wahoo, Great barracuda, Skipjack tuna, Yellowfin tuna, Giant trevally, Lantern fish, Deepwater snapper

A Bull shark

R² = 0.70
p < 0.001

B Tiger shark

R² = 0.31
p < 0.001

muscle δ^{202}Hg (‰)

Length (cm)

iHg

EPIPELAGIC NEARSHORE

MDF

Bull shark
Δ^{199}Hg = 2.1 ‰
δ^{202}Hg = 1.9 ‰

iHg

EPIPELAGIC OFFSHORE

MDF

Skipjack tuna
Δ^{199}Hg = 2.3 ‰
δ^{202}Hg = 0.5 ‰

Giant trevally
Δ^{199}Hg = 2.1 ‰
δ^{202}Hg = 0.6 ‰

MeHg

MIF

MESOPELAGIC NEARSHORE

MDF

Tiger shark
Δ^{199}Hg = 1.8 ‰
δ^{202}Hg = 1.2 ‰

iHg

MESOPELAGIC OFFSHORE

MDF

Lantern fish
Δ^{199}Hg = 1.9 ‰
δ^{202}Hg = 0.5 ‰

Deepwater snapper
Δ^{199}Hg = 1.8 ‰
δ^{202}Hg = 0.2 ‰

MeHg

iHg   *MDF*   MeHg

Twilight zone

Figure captions

Figure 1: Map of sampling locations of the shark and prey species along the west coast of La Réunion Island. Major rivers are figured in white lines. Lantern fish are not shown but were caught in the area (off La Réunion Island and off southern Madagascar).

Figure 2: A: Δ^{199}Hg (‰) in the bull shark (orange bar, mean ± SD), the tiger shark (green bar, mean ± SD) and prey species (dots, mean ± SD) from La Réunion Island. The prey fish are ordered according to their Δ^{199}Hg values. The bull shark had higher (ANOVA, $p < 0.001$) Δ^{199}Hg than the tiger shark. The bull shark shared similar Δ^{199}Hg with the yellowfin tuna and the giant trevally while the tiger shark shared similar Δ^{199}Hg with the deepwater snapper.
B: δ^{202}Hg (‰) in the bull shark (orange bar, mean ± SD), the tiger shark (green bar, mean ± SD) and prey species (dots, mean ± SD). Bull shark had higher (KW, $p < 0.001$) and more variable (Bartlett test, $p < 0.001$) δ^{202}Hg than tiger shark. Bull shark had higher δ^{202}Hg than its prey (e.g. giant trevally; KW, $p < 0.001$). Similarly, the tiger shark displayed higher δ^{202}Hg than its prey (e.g. deepwater snapper; ANOVA, $p < 0.001$).

Figure 3: Muscle δ^{202}Hg values versus total length for the bull shark (**A**) and the tiger shark (**B**). Data fits a linear regression in A and B.

Figure 4: Simplified representation of the Hg cycle in the environment of bull and tiger sharks. Atmospheric inorganic Hg (iHg) is deposited to water before being methylated to methyl-Hg (MeHg) along the water column, which induces mass-dependent fractionation (MDF). MeHg can then be demethylated by solar radiation in the photic zone of the water column, inducing mass-independent fractionation (MIF). Hg can reach the deep layers trough particle sinking, either in the MeHg form, or in the iHg form. iHg can also be methylated in the twilight zone. Epipelagic MeHg is directly incorporated into the bull shark food web, while the tiger shark food web is exposed to a mixed pool of (i) mesopelagic offshore MeHg and (ii) benthic MeHg subject to bacterial transformation in slope sediments. MeHg is finally demethylated in sharks, leading to high δ^{202}Hg values. Reduction of iHg into gaseous Hg^0 and subsequent volatilization is not represented.

Highlights:

Mercury isotopes were analyzed in bull and tiger sharks from the Indian Ocean

Hg MIF signature revealed that bull sharks target coastal prey in shallow water

Δ^{199}Hg values showed that tiger sharks forage on deeper habitat on the island slope

δ^{202}Hg shift between prey and predator may indicate MeHg demethylation in sharks

Declaration of interests

☒ The authors declare that they have no known competing financial interests or personal relationships that could have appeared to influence the work reported in this paper.

☐ The authors declare the following financial interests/personal relationships which may be considered as potential competing interests: